NASA

Technical Memorandum 85062

The Inner Edge of the Plasmas Sheet and the Diffuse Aurora

D. H. Fairfield and A. F. Viñas

JUNE 1983

National Aeronautics and
Space Administration

Goddard Space Flight Center
Greenbelt, Maryland 20771

THE INNER EDGE OF THE PLASMA SHEET AND THE DIFFUSE AURORA

D. H. Fairfield and A. F. Viñas
NASA/Goddard Space Flight Center
Laboratory for Extraterrestrial Physics
Greenbelt, Maryland 20771

ABSTRACT

Three dimensional measurements from the ISEE-1 low energy electron spectrometer are used to map the location of the inner edge of the plasma sheet and study the anisotropies in the electron distribution function associated with this boundary. Lower energy plasma sheet electrons have inner edges closer to the earth than higher energies with the separations at different energies being larger near dawn and after dusk than at midnight. Lowest energy inner edges are frequently located adjacent to the plasmapause in the dawn hemisphere but are often separated from it in the dusk hemisphere by a gap of at least several R_e. The energy dispersion is minimal in the afternoon quadrant where the inner edge is near the magnetopause and frequently oscillating on a time scale of minutes. The location of the inner edge is probably determined primarily by the motion of electrons in the existing electric and magnetic fields rather than by strong diffusion as has sometimes been supposed. Evidence against strong diffusion is: (1) boundaries closer to the earth than would occur if strong diffusion were operating and (2) the frequent and persistent occurrence of anisotropies that would be rapidly smoothed if pitch angle scattering proceeded at the strong diffusion rate. These anisotropies include 90° pitch angle depletions at the inner edge and 90° enhancements in the surrounding regions. Both these anisotropies are predicted by calculations of single particle motion; the former are apparently due to more field aligned particles having inner edges slightly closer to the earth than 90° particles and the latter are apparently due to the preferential adiabatic acceleration of 90° particles drifting in cross-tail electric and dipole-like magnetic fields. These anisotropic distribution functions created by normal particle motion contain free energy which may be that necessary to drive the electrostatic electron cyclotron instabilities thought to be responsible for generating the waves that preciptate particles of the diffuse aurora. An additional cool component of the plasma is also observed which should also influence these instabilities.

Introduction

A dawn-dusk electric field across the magnetotail is thought to be the fundamental driving mechanism for most magnetospheric processes. This electric field causes particles of the magnetotail plasma sheet to convect earthward until the increasing influence of the co-rotating geomagnetic field diverts the flow and causes it to continue around the earth and out the front of the magnetosphere. In this manner a boundary is formed between the relatively hot tenuous plasma from the magnetotail and the cool dense plasmasphere which co-rotates with the earth and is supplied by the ionosphere. This simple picture is complicated by the transport of particles between the ionosphere and magnetosphere on a great variety of time scales and by time variations of all the various processes that are involved. The observational picture has remained somewhat clouded, particularly the relation between the inner edge of the plasma sheet and the plasmapause.

Observations from the OGO spacecraft in highly excentric orbits indicate that the inner edge of the plasma sheet is frequently adjacent to the plasmapause near and after midnight, but not necessarily before midnight. Frank (1971) found correspondence of these boundaries in each of 7 post-midnight cases but he found the inner edge 1-3 R_e beyond the plasmapause in 7 of 10 pre-midnight cases. In the local time region from 17-22 hours Vasyliunas (1968a) found that the earthward termination of the plasma sheet near the equatorial plane is near 11 R_e during quiet times and closer to the earth during magnetic substorms. This 11 R_e boundary would appear to be well beyond the plasmapause but there are few direct comparisons in this region. Another important observation is that the boundaries of lower energy electrons are invariably closer to the earth than those at higher energies (Schield and Frank, 1970; Frank, 1971). When comparing boundary observations made at different times it is usual to suppress this additional complication and discuss a boundary near one keV which is not appreciably outside the zero energy boundary.

In the dawn to noon quadrant Vasyliunas (1968b) found relatively intense plasma sheet fluxes extending inward from the magnetopause which have no clear inner boundary. Recently, however, Horwitz et al. (1982) have studied 14

passes of ISEE 1 in the dawn hemisphere. Using a sensitive indicator of the plasmapause they consistently find a concurrent plasmapause and inner edge with a location which is generally in the range L = 4-6.

At local times earlier than 1700 Vasyliunas (1968b) reports a situation in the outer magnetosphere that is dramatically different from the dawn hemisphere. In this noon-dusk region the inner edge is found at the same 11 R_e distance that it occurs at later local times. This location implies that the plasma sheet is confined to a region of decreasing thickness between the magnetopause and 11 R_e as the magnetopause moves closer to the earth at these earlier local times. This plasma sheet of diminishing thickness was found to finally disappear at a local time that varies from day-to-day but is approximately at 1300. Fluxes between the inner edge and the plasmapause were generally undetectable near dusk and increased gradually toward noon such that they merged with the intense pre-noon fluxes.

Additional measurements of the plasma sheet inner edge near the equatorial plane have been made by spacecraft in or near synchronous orbit. Such spacecraft can only see the inner edge when it is within this radial region and consequently the emphasis in analyzing this data has been on time dependent accelerations and the plasma motions that bring it to this location. Examples of synchronous spacecraft motion through an energy dependent boundary in the dusk quadrant have been cited as confirmation of the essentially equilibrium picture where various energies have their own inner boundaries (e.g., Kivelson et al., 1980; Hultquist et al., 1982). Mauk and Meng (1983) find anomalous energy dispersion as the Scatha spacecraft moves inward from the plasma sheet in the noon-dusk quadrant and they question the equilibrium picture even during quiet times. Even their frequent observation of inner edges in the range L = 5-8 seems to conflict with the more distant locations reported by Vasyliunas.

At low altitudes extensive measurements have been made of a sharp low latitude boundary to auroral electrons which can be observed both optically (e.g., Sheehan and Carovillano, 1978) and in precipitating electrons (e.g., Gussenhoven et al.,1981). Existing data (Meng et al., 1979; Slater et al., 1980; Horwitz et al., 1982) support the commonly made assumption that this low

altitude boundary corresponds to the inner edge of the plasma sheet. Comparisons of particles and aurora with ground determinations of the plasmapause are also in reasonable agreement with the overall picture. Foster et al. (1978) found that precipitating electrons were adjacent to the plasmapause near dawn but were well poleward of the plasmapause near dusk. However, he also cited some evidence that trapped plasma sheet electrons at dusk were present adjacent to the plasmapause, an observation which may be inconsistent with outer magnetosphere measurements. Linscott and Scourfield (1976) discuss one case during a disturbed period when the diffuse aurora were adjacent to the plasmapause in the dusk to midnight quadrant.

A considerable amount of theoretical work has been undertaken in an effort to quantitatively explain the inner edge of the plasma sheet and the generation of the diffuse aurora. It is generally agreed that some instability generates waves - most probably electrostatic electron cyclotron waves (e.g., Swift, 1981 and references therein) - which pitch angle scatter plasma sheet electrons into the loss cone. What conditions lead to instability and what determines the location of the inner edge is less clear, but the alternative answers to the latter question follow either of two approaches.

The first approach (Kennel,1969, Southwood and Wolf,1978; Ashour-Abdalla and Kennel, 1978; Kennel and Ashour-Abdalla, 1982) is based on the assumption that strong diffusion is the cause of the particle precipitation. Under this assumption particle distributions are quite isotropic and the lifetime approaches a minimum lifetime $T_m = 2T_b/\alpha_o$ squared where T_b is the quarter bounce time of a particle moving along an auroral field line and α_o is the equatorial loss cone angle. Assuming a dipole field, $T_m = L^4/(E_e)^{1/2}$ where E_e is the electron energy and L is the conventional L parameter. It is further argued that the characteristic flow time for earthward particle convection is $T_f = 10^7/L^2\phi$ sec where ϕ is the electric potential across a 40 R_e wide magnetotail in kilovolts. Far from the earth, particle lifetime T_m is very long compared to T_f and the particles convect earthward with very few being lost. At smaller L, however, a point is reached where the lifetime, which is decreasing as L^4, is small compared to the time T_f in which the particles convect an incremental distance earthward and which is increasing as $1/L^2$. At

this point most particles precipitate and the inner boundary results. The location of the boundary is energy dependent, because of the inverse dependence of T_m on energy, and the lower energies move further earthward as is observed. The intersection of the T_m and T_f curves occurs at roughly 7-10 R_e with larger potentials corresponding to closer distances, so agreement with Vasyliunas's early measurements of 11 R_e boundaries was thought to be satisfactory.

A second theoretical approach is based on calculations of the motion of individual particles in a dipole magnetic field and a model electric field (Kavanagh et al., 1968; Kivelson and Southwood, 1975; Southwood and Kivelson, 1975; Cowley and Ashour-Abdalla, 1975, 1976; Ejiri, 1978; Southwood and Kaye, 1979). Particle diffusion is not considered, at least initially. Results of such calculations show how zero energy particles follow the electric equipotentials as they convect earthward from the tail and are excluded from the closed region near the earth thought to be the plasmasphere. Higher energy electrons also convect earthward but in addition they also undergo eastward magnetic drifts which are proportional to their energy. This additional velocity moves them around the earth faster than the low energy particles and they fail to penetrate as close to the earth as the low energy electrons. In this manner each energy develops its own inner boundary. Theoretical inner boundaries for 0, 1, 2, and 7 keV electrons are illustrated in the equatorial plane view in Figure 1. Note that particles gain energy as they drift so these curves do not exactly correspond to drift trajectories (Alfvén layers). Theory (Cowley and Ashour-Abdalla, 1975; Ejiri, 1978) also indicates that field aligned particles penetrate somewhat closer to the earth and the shaded region indicates the separation between 0/180° and 90° pitch angles at each energy. Figure 1 has been prepared using the formulation of Southwood and Kaye (1979) for a co-rotation electric field plus a uniform cross tail electric field of .95 kev/R_e. The dusk symmetry point has been rotated by -8° (toward the sun) to agree with measurements on a particular day that will be presented in Section 3. Large cross-tail fields should convect particles deeper into the magnetosphere and this fact has been used in the interpretation of the resulting boundaries to obtain values of the magnetospheric electric field (Berchem and Etcheto, 1981; Hardy et al., 1981; Hultqvist et al., 1982; Nakai and Kamide, 1983). While undergoing magnetic drift motions the particles are

energized as they move in the cross-tail electric field and the electrons with pitch angles nearer 90° are energized more than field aligned particles. To the extent that this single particle approach is valid, this effect will tend to produce $T_\perp$ greater than $T_\parallel$, an anisotropy which is a possible free energy source for an instability that might generate waves to provide the pitch angle scattering (Ashour-Abdalla and Cowley, 1974). This point will be pursued in Section 4.

These two theoretical approaches have fundamental differences. The former follows from the assumption of strong diffusion although this condition can be relaxed somewhat (Southwood and Wolf, 1978). It claims that the inner boundary is the result of particle depletion via precipitation. The latter is based on the validity of single particle motion (unaffected by diffusion) and it claims the inner edge is simply due to where particles move in the assumed magnetic and electric fields. A weakness of the latter approach is that it does not take into consideration collective effect such as currents and pressure gradients which modify the electric and magnetic fields assumed initially. A weakness of the former approach is that strong diffusion is an unproven hypothesis. Neither approach should be viewed as an exclusive answer, since on the one hand the single particle approach ultimately invokes diffusion to precipitate the particles and on the other hand the equations governing particle motion are certainly acting even if diffusion is dominant. The role of experiments must be to determine the times and places when one process or the other is more important. If the boundary is observed at a greater distance than that predicted by the single particle Alfvén layer calculations, this would suggest that the boundary is caused by precipitation before the particles have a chance to penetrate to where they would in the absence of diffusion. If the boundary is found at the location predicted by single particle calculations and this location is inside the boundary predicted by strong pitch angle diffusion, this would indicate that the diffusion is not as strong as assumed. In reality such tests are not straight forward because the single particle predictions are for a steady state based on a simple electric field model whereas actual boundaries are determined by variable electric fields which are undoubedly more complex than the models.

In the present work we have undertaken a survey of the first 15 months of ISEE 1 low energy electron measurements in an effort to more clearly delineate the location of the inner edge and understand why it is located where it is. On the basis of this inner edge location and anisotropies in the three dimensional distribution function, we will argue that strong diffusion is frequently not in effect. Various predicted effects of single particle motion are observed and the resulting anisotropies may be a source of free energy for the waves precipitating particles of the diffuse aurora.

Instrument and Data Reduction

The electron spectrometer experiment on ISEE 1 (Ogilvie et al., 1978) measures the three dimensional electron distribution function during individual 3-second spacecraft rotations. Six individual sensors with 8.5° x 11° viewing angles are mounted to form two triaxial spectrometers. The axes of each spectrometer are orthogonal and the look directions of one spectometer are exactly opposite to those of the other spectrometer. The six sensors are simultaneously sampled in at logarithmically spaced energies extending over a range which is set to either 11 eV to 2.06 keV or 109 eV to 7.28 keV in the magnetosphere-magnetotail. Each energy sweep takes 0.5 s or 1/6 of a spacecraft spin. As the spacecraft spins the individual sensors, which make angles of ± 16.2 , ± 31.7, and ± 53.5 with the spacecraft equatorial plane, sweep out 6 spatial bands on the unit sphere while they are each undergoing 6 energy sweeps. Thus each energy is sampled 6 times by each of 6 detectors giving 36 widely separated points on the unit sphere, half of which are located diametrically opposite to another simultaneously sampled point. In the high (low) bit rate mode every third (sixth) 3 s spin is sampled giving complete data sets every 9 or 18 s.

Moments of the electron distribution function have been routinely calculated for the 15 months following the October 1977 launch of ISEE 1 into an orbit with apogee 23 R_E and orbital period 2.4 days. A return current relationship is invoked to calculate the spacecraft potential (similar to that in Scudder et al., 1981) and a correction of the measured energies is made using this potential.

It has also proven useful to plot the electron distribution function, f, at each energy as a function of time. More specifically, we calculate the average f for all measurements with pitch angles 90° ± 30° and plot this quantity $f_\perp$ along with the average $f_\parallel$ for all the remaining f values having pitch angles within 60° of the parallel or anti-parallel field direction. (Pitch angles are calculated using the 1 minute $\vec{B}$ data from the experiment of C. T. Russell obtained via the ISEE data pool tapes.) ISEE usually assumes a positive potential in the low density plasma of the magnetosphere and magnetotail and with such plots it is generally possible to identify the contaminating electrons of the spacecraft photoelectron sheath. With such information it is possible to eliminate the contaminating data and recompute moments with greater accuracy.

Position of the Inner Edge

A prominent feature on the plots of log f vs time is the flux change that marks the inner edge of the plasma sheet. As the spacecraft moves inward, higher energies invariably decrease at greater distances from the earth than the lower energies, with the separation ranging from a fraction to a few earth radii. An example of such data is shown in Figure 2 where log f values for the 14 highest energy channels in the lower energy mode are plotted vs time on July 17, 1978. Dots represent $f_\perp$ and lines represent $f_\parallel$ and only every third available point is plotted to prevent overcrowding. In Figure 2b we show the moments and the magnetic field for the same interval. As the spacecraft moves earthward near 2000 LT a flux decrease is seen first in the highest energy $f_\perp$ values at about 0330 UT and then seen later at lower energies. The earlier decrease in $f_\perp$ is an indication of the more earthward penetration of field aligned particles which will be discussed further in the next section. The high energy decrease is reflected as a cooling of the electrons between 0300 and 0400 with little density change. The locations of the inner edges at 2 keV, 1 keV and at low energies on July 17 are shown by the points in Figure 1. Taking these locations along with those for intermediate energy channels, we have used an inversion technique based upon a constrained non-linear least square method to determine the convection electric field E and its orientation angle ψ_o. The model used was the co-rotation plus uniform cross tail electric field and dipole magnetic field used by Cowley and Ashour-Abdalla (1976), and

Kivelson and Southwood (1975) with the exception that a orientation angle for the electric field was included as an additional parameter. The procedure involved minimizing the norm of the difference of $||L_A^o - L_A(W, \alpha, \psi, E, \psi_o)||$ where L_A^o is the set of observed locations, L_A are the model predictions, and W is particle energy, α is pitch angle, and ψ is local time. The procedure involved iterating until an optimum solution is obtained for the model parameters E and ψ_o (.95 keV/R_e and -8° (clockwise) in the present case). A fundamental limitation of the technique is the assumption that a steady state has been reached and persists throughout the period of the measurements. These E and ψ_o values are also used in the model to produce the smooth curve cutting through the inner edges in Figure 2.

An example from the dawn to noon quadrant is shown in Figure 3. Again we see an energy dependent inner edge centered on approximately 1430 UT. Another prominent feature seen in this local time region and illustrated by Figure 3a is the enhancement of fluxes at pitch angles near 90° as is indicated by the displacment of the $f_\perp$ dots above the $f_\parallel$ lines at all energies. This enhancement of $f_\perp/f_\parallel$ is characteristic of virtually every pass through this region and is especially prominent for locations within about 20° of the equatorial plane. This anisotropy leads to a clearly defined axis of the pressure tensor which agrees very well with the measured magnetic field direction as is illustrated by the correspondence of the traces in the bottom panel. The best fit uniform electric field is .58 keV/R_e with the pattern rotated -12°. These are very reasonable values for this very quiet day.

Inner edges seen in the noon to dusk quadrant are usually of a different character than those in other regions. An example from September 5, 1978 is shown in Figure 4. The inbound spacecraft crosses the magnetopause at 0504 as can be deduced from the density decrease and the transition to a magnetosphere-like magnetic field orientation. Hot plasma sheet electrons are present inside the magnetopause except for a brief interval of cooler denser boundary-layer-like plasma for a few minutes around 0515. Fluxes of hot electrons have disappeared by 0630 but there is considerable variability in the fluxes from 0530 to 0630 suggesting considerable motion or structure of this inner boundary. On some days such as at 0612 in Figure 4a, energy dispersion is detectable (i.e., the intervals of high flux are of longer

duration for lower energies as would be expected if the lower energies extended in closer to the earth). Energy dispersion implies that boundary movement is more likely than structure. September 5 electric field data (A. Pederson, private communication) appears to vary with the same frequency and phase as the hot particles come and go, which also suggests wave-like motion of this boundary. Notice that on this day the spacecraft has only moved inward from the magnetopause by 1.5 R_e by the time the fluxes disappear, and they are variable throughout most of this interval. This morphology is very typical of the noon-to-dusk region and it confirms the picture of Vasyliunas where plasma sheet electrons are confined to a relativly narrow region inside the afternoon magnetopause.

In instances when data coverage is unusually continuous we are sometimes able to observe the inner edge of the plasma sheet on inbound and outbound passes that are only a few hours apart in elapsed time. When geomagnetic activity is quiet or unusually steady over this interval we can hope to compare these locations. Such a case is illustrated with high energy mode data in Figure 5 on February 11-12 1978, a period of extreme quiet only marred by one small AE < 200 nT disturbance 2 - 4 hours before the first crossing. Here the inbound inner edge is seen at 2100 UT and 0600 LT and the outbound inner edge is seen at 0027 UT and 2400 LT. (The flux increase near 2130 and the subsequent decrease are due to penetrating particles of the outer radiation belt - an observational problem whose effects will be discussed below.) Note that the midnight plasma sheet is cooler and plasma sheet particles are only seen up to 5 keV. The dawn plasma sheet is considerably hotter (2.2 keV vs 600 eV at midnight) because particles are accelerated as they drift in the cross-tail field. At midnight during this quiet period we have the unusual situation where 7 keV fluxes in the more earthward "forbidden" region are actually higher than those of the plasma sheet, so a decrease is seen at the inner edge. This example reinforces the idea that we are indeed dealing with a boundary separating particles with different sources or different histories. Note that if we had been in the lower energy mode observing energies less than 2 keV the inbound pass would have been less apparent since it would have been detectable only in the highest 4 or 5 channels.

The characteristic separation of inner edges at various energies is also illustrated in Figure 5. Almost 2 hours are required to see the flux decrease shift from 7 keV to 500 eV as the inbound spacecraft moves fairly slowly from 8 to 5 R_e near the dawn equatorial plane whereas only 4 minutes are required for the outbound spacecraft to cut the inner edges on L shells of 7.7 to 8.0 near local midnight. This shorter duration near midnight is due partly to the fact that the spacecraft is moving more rapidly at 4.7 R_e and 38° magnetic latitude. Also the 7 keV boundary extends quite far out in the magnetosphere near dawn, but this boundary is absent near midnight. In spite of the above effects there appears to be a real enhanced separation in the boundaries near dawn compared to midnight. This is further illustrated in Figure 6 where the separations of the boundary crossings at different energies are plotted vs local time. In the dawn and dusk regions the boundaries are invariably separated by 1 R_e or more whereas near midnight the separation is seldom more than a few tenths of an R_e. The separations may be over-estimated by as much as 30% in the dusk region because these inbound passes cut an azimuthally dependent boundary at an oblique angle, but the dawn passes are nearly normal to the boundary. In contrast to observations, the theory for a uniform cross tail field predicts that the energies would have their minimum separation near the dawn meridian. More sophisticated electric field models are usually expressed by a potential

$$\phi = CL^{\kappa} \sin\Psi - 91/L$$

where C is a constant and Ψ is a local time angle. $\kappa = 1$ reduces to the uniform field model and larger κ's yield electric fields which decrease more rapidly near the inner edge. The boundaries predicted by higher κ's are more circular with less of a dusk bulge, but they do not predict an increasing separation of energies near dawn. This enhanced separation may be related to the importance of shielding (e.g., Southwood and Wolf, 1978) or perhaps it needs to be explained by a more sophisticated model such as that of Mauk and Meng, 1983).

To compile a statistical picture of the inner edge we have surveyed 160 of the first 180 orbits of ISEE 1 electron data. The inner edge was determined with reasonable confidence on 49 outbound passes and 47 inbound

passes. When an inner edge was not found, this lack could generally be attributed to missing data, contamination from energetic penetrating radiation, or confused profiles which were often due to time variations during especially disturbed times. To facilitate presentation and comparison with other measurements, we focused on boundaries at the single energy of 1 keV. This 1 keV boundary is located only slightly beyond the zero energy inner edge yet it is an energy where the inner edge is invariably observed and for which we have very similar energy channels in both our high and lower energy modes.

In Figure 7a we show the equatorial plane view of the observed locations of the inner edge at 1 keV on quiet days. Quiet days are defined by AE < 100 nT (Kp < 2- in 1977 when AE was not available), where values are averaged over the 6 hour interval including and prior to the measurement. Solid circles indicating the inner edge and crosses indicating the magnetopause are connected by spacecraft trajectory lines on inbound passes which tend to be fairly near the equatorial plane (latitude < 20°). Open circles indicate inner edges on outbound passes which generally occur at higher latitudes and lower altitudes. For these high latitude observations the L value of the inner edge is plotted at the appropriate solar magnetospheric longitude. For the inbound equatorial measurements the positions have been rotated to the equatorial plane in a meridian plane. More points appear in the dawn hemisphere since data from the fall of both 1977 and 1978 are included. Dashed lines indicate the average locations of low latitude boundaries in precipitating electrons detected on the DMSP spacecraft at low altitudes (Gussenhoven et al., 1981, 1982) which have been projected to the equatorial plane using the Mead-Fairfield magnetic field model (Mead and Fairfield, 1975). The inner and outer lines are averages for Kp = 0 and Kp = 1 respectively. A circle is drawn at the 6.6 R_e synchronous orbit distance for reference. A clear dawn-dusk asymmetry is the main feature of the data with the dawn points occuring mostly between 5 and 7 R_e and dusk points falling mostly beyond 10 R_e. For these quiet times there is rather good agreement between the ISEE points and those from low altitudes. The inner edge is frequently beyond the synchronous orbit during quiet times, especially in the dusk and dayside regions.

Figure 7b illustrates similar data for the more disturbed conditions not included in Figure 7a. Open circles again represent outbound passes and heavy solid circles represent inbound passes, but in addition the quiet time points from Figure 7a have been included as smaller dots to facilitate comparison.

In the noon-to-dusk quadrant the positions are not very different from the quiet days. These data confirm the picture of Vasyliunas (1968b) where the inner edge is relatively far out and near the magnetopause in the noon-dusk quadrant. From the length of the trajectory segments it can be concluded that the plasma sheet is typically 1-3 R_e thick between 14 and 17 LT and it becomes thinner near noon. Again we emphasize that inner edges in this quadrant show relatively little energy dispersion and frequently appear to be oscillating rapidly on a scale of minutes.

In the dawn-to-noon quadrant the situation contrasts sharply with that near dusk. In this pre-noon region during disturbed times, high count rates are detected in to approximately 3 R_e and inner edges are not apparent. These missing boundaries are thought to be related to the high counting rates present inside 4 R_e which are due to energetic particles of the radiation belts which penetrate the detector and produce an abnormally high background. When the cross tail electric field is enhanced the plasma sheet particles move inward and merge with the region of contaminating counts, thus eliminating any flux decrease that would identify the inner edge. During more quiet times the inner edge is further out and separated from the inner region of high background counting rates. Gussenhoven et al. (1981) have noted a similar problem with penetrating radiation in their low altitude data. Vasyliunas (1968b) did not find inner edges in this region, however we find clear inner edges during more rare quiet conditions.

In the midnight hemisphere the dawn-dusk asymmetry is the predominant effect for all conditions. There also appears to be a tendency for the outer magnetosphere data to fall outside the projected low altitude data in the dusk-to-midnight quadrant. This is probably due at least partly to the fact that the Mead-Fairfield model undoubtedly underestimates the field line distortion at 5 - 7 R_e in the dusk-to-midnight quadrant; the low altitude data should probably be projected further out into the magnetosphere in this

region. It would be surprising if this were the entire explanation, however, especially in the noon-to-dusk quadrant where an extrapolation of the low altitude data would appear to be well inside the outer magnetosphere data.

An explanation for this discrepancy can be postulated after considering a likely model of the overall convection pattern. Figure 8 is a qualitative summary figure prepared by adapting Figure 2 of Vasyliunas (1968b). The limited thickness of the plasma sheet in the noon-dusk region is undoubtedly due to plasma convecting sunward from the dusk portion of the magnetotail. Plasma traversing the earth via dawn is also expected to arrive in the noon dusk quadrant after drifting duskward through noon. This plasma will have supplied the diffuse aurora throughout its transit and will be depleted in intensity by the time it passes through noon. The more tenuous plasma may be below the detection threshold of ISEE and OGO which then, by default, will identify only the more prominent boundary of the sunward flowing plasma near the magnetopause. Low altitude spacecraft may be able to detect the weaker, but more equatorward boundary of the electrons arriving via dawn. Even though the latter plasma may be more tenuous it is possible that it is precipitated more efficiently than the higher latitude plasma. Some support for the above explanation is provided by the two most earthward quiet day inner edges near 1500 LT in Figure 7a. These crossings exhibit the clear smooth energy dispersion characteristic of the other three local time quadrants rather than the highly variable fluxes more commonly seen further out near the magnetopause. Perhaps on these quiet days the inner edge to the plasma arriving via dawn was further out and less depleted by loss and detectable by ISEE.

The Electron Distribution Function Near the Inner Edge

To help understand the cause of the diffuse aurora and the location of the inner edge of the plasma sheet it is useful to investigate the shape of the distribution function as a function of velocity and pitch angle. In this section we will illustrate the unique pitch angle distributions commonly seen at the inner edge of the plasma sheet and comment on the shapes of the distribution functions arising from them.

The most dramatic pitch angle distributions are seen near the inner edge of the plasma sheet in the dusk-to-midnight quadrant. A typical example from this region is shown in Figure 9 where f is plotted vs pitch angle for the various energy channels. Each panel contains data from an individual spacecraft spin on the inbound pass on June 20, 1978 during a period of moderate disturbance (AE = 200 nt). Data correspond to times when the spacecraft was crossing the inner edge at energies of 1.03 keV, and 724, 510, 359,and 255 eV respectivly. In each panel the energies below this transition energy (those toward the top of the figure) have fluxes characteristic of the plasma sheet whereas those at higher energies exhibit lower fluxes characteristic of the region earthward of the inner edge. The energy whose inner edge is being crossed exhibits an unusual pitch angle distribution where fluxes at the high and low pitch angles remain high while those near 90° have decreased to their lower values. This effect often produces large values of $f_{\parallel}$ relative to $f_{\perp}$ such as is seen near 0400 in Figure 2. This pitch angle dependence is apparently that predicted by single particle theory and illustrated in Figure 1 whereby the high/low pitch angle electrons penetrate closer to the earth than those at 90°. This effect is dramatically evident on each of the 5 equatorial inbound passes seen in the local time region between 2000 and 2400 LT. Such data are illustrated with Figure 10 which shows 510 eV inner edge crossings on four different days. The right hand panel, which is a repeat of the center panel of Figure 9, is clearly similar to the inner edge crossings on the three other days. There are differences in how rapidly the 510 eV fluxes make their transition from high to low values and the June 8 decrease is not so dramatic at this energy, but diffusion will tend to smooth this transition and it is significant that it can be as abrupt as it is.

Another common characteristic of plasma sheet pitch angle distributions near the inner edge is a tendency for maximum fluxes to occur at 90°. This effect is also predicted by the theory of single particle motion in a dipole magnetic field and cross tail electric field; 90° electrons are expected to be accelerated more than high/low pitch angle electrons as they drift toward dawn (Cowley and Ashour-Abdalla, 1975). The 359 eV channels in panels a, c and d in Figure 10 illustrate this effect. Panel b fails to show the effect at this energy but similar peaks at other times on this day will be discussed below.

Apparently two different processes are at work shaping the distribution function near the inner edge. One increases 90° particles at various energies over a broad spacial region while the other selectively excludes 90° particles in favor of field aligned particles at the inner edge. The simultaneous occurence of both these processes seems to be occurring at the time of the data shown in Figure 11. Panel a of these pitch angle plots occurs at the time of the inner edge crossings at the highest energy (2.06 keV). A peak is seen at 90° at this energy but it appears as if the peak were superposed on a distribution that would otherwise be decreasing near 90°. In successive panels taken over the next few minutes, this characteristic shape spreads to lower energies as inner edges are crossed at 1.46 keV, 1.03 keV and 724 eV. In panel e the spacecraft apparently has moved in far enough to be inside the 90° enhanced fluxes at 510 eV but in panel f they are again superposed at 359 eV.

An experimental determination of the distance between the 0° and 90° boundaries is precluded by the motion of the boundaries that can be as large or larger than the spacecraft velocity. The separations certainly do not seem to be inconsistent with the few tenths of an R_e separation of the 0° and 90° boundaries indicated by Figure 1.

In the region near dawn the pitch angle distributions have similar characteristics to the nightside distributions discussed above but the 90° exclusions are not seen as consistently or dramatically. Figure 12 shows pitch angle distributions on February 14, 1978. The experiment was in the high energy mode which is more appropriate for the hotter plasmas typically seen near dawn. The several panels again correspond to times when the inbound spacecraft crossed the inner edges at various energies. Beginning with panel a when the 4.1 keV inner edge was being crossed, one again sees a slight depression at 90° which moves to lower energies in subsequent panels as the inner edge is crossed at lower energies. At energies below this transition energy the distribution is peaked at 90°. At dawn this 90° enhancement is usually more prominent than near midnight, perhaps because the inner edges, tend to occur nearer the earth where the plasma has convected further into the dipole-like magnetic field. An especially prominent enhancement at 90° at low energies can also be seen in Figure 12. This is frequently seen in the dawn

hemisphere near the equator and is apparently the phenomenon noted by Wrenn et al. (1979).

In searching for plasma instabilites that might generate waves which would precipitate the electrons causing the diffuse aurora, it is useful to investigate the plasma distribution function in velocity space. In the upper panels of Figure 13 we show contours of the distribution function with $v_{\parallel}$ the horizontal axis and $v_{\perp}$ the vertical axis. In the lower panels we show orthogonal cuts through the distribution function where the horizontal axis is $v_{\parallel}$ or $v_{\perp}$ for the heavy and light lines respectivly. Data from three spins is shown corresponding to panels c, e and f in Figure 11. The left hand panel in Figure 13 has contours which are somewhat elongated in the parallel direction with a secondary enhancement in the perpendicular direction corresponding to the central peak in Figure 11c. The center panel has more elongated contours at higher energies due to the extreme drop in 90° particles near the inner edge. In the right hand panel the elongation in the parallel direction is still more extreme as additional energies and pitch angles have decreased. The degree of elongation is more clearly illustrated by the bottom panels which show that $f_{\parallel}$ can exceed $f_{\perp}$ by more than an order of magnitude.

Another feature to note in Figure 13b is the secondary indentation in the contours near the field direction at a velocity near 1.5×10^9 cm/s. This is caused by the fact that f at 15° pitch angle and 510 and 359 eV energy is lower than f at 30° (see Figure 11e). When this data is interpolated to produce the contours at $v_{\perp} = 0$, the indentation is produced. This indentation is significant because it is indicative of a region of $df/dv_{\perp} > 0$ which is a condition for instability (e.g., Kennel and Ashour-Abdalla, 1982). Such a decrease could be indicative of a loss cone, but at this time in the distant magnetosphere the loss cone is only 1.2° wide, an angle that is very small compared to our 8.5° x 11° viewing angle. It is important to know if the loss cone is empty because if it is: (1) it confirms that strong diffusion is not operating and therefore is not responsible for producing the inner edge of the plasma sheet, and (2) there will be a region of positive $df/dv_{\perp}$ to cause an instability and create waves which would precipitate electrons. To further investigate this question we can look at outbound ISEE passes when the inner edge is traversed at low altitudes where the loss cone is of comparable size to our viewing angle.

Figure 14 shows distribution function contours and projections along with pitch angle distributions near the inner edge on three different days. Each example came from the local time region 2200-2400 and the radial distances were 3.4, 4.9, 2.7 and L values 4.3, 8.2, and 4.3 respectively. In the strong fields at these low altitudes the loss cone angles are 7.7°, 4.9° and 11.7° and hence fill a significant portion of the experiment viewing angle when the detector is aligned near the field direction. In panel a it is clear that a substantially reduced f value is measured at the pitch angles nearest the field direction. A similar depression in the loss cone at much lower altitudes has been reported by Sharber (1981). Our low values occur at the middle energies because in this example a detector happened to be measuring these energies as the spacecraft spin swept it nearest the field direction; higher and lower energies might have had similar distributions but comparably high/low pitch angles were not measured. The top panels show a substantially reduced $f_{\parallel}$ relative to $f_{\perp}$ and the contours show an abrupt indentation near the field direction which would clearly lead to a positive value of $df/dv_{\perp}$. Panel b corresponds to the example of Figure 5. In this case the most field aligned electrons are measured near 2 keV and the f depression appears to be larger for those particles moving away from the ionosphere (180°) than those moving earthward (0°). This case is what one might expect if strong diffusion were operating near the equatorial plane, but this is by no means the typical situation. Note that the more depressed pitch angle distributions near 180° correspond to the more indented contours on the left side of the panel above. Panel c shows an intermediate case where the f's are moderately depressed near 0° and 180°, but perhaps slightly more for the 180° upcoming electrons. Horwitz et al. (1982) demonstrate that ISEE-1 has indeed just passed from the plasmasphere into the plasma sheet at this time and is on field lines connecting to the diffuse aurora. The sensitivity of the contour plots is indicated by the flat portion of the $f_{\parallel}$ cut at $v_{\parallel} = 2 \times 10^9$ cm/s and the small circlular contour on the $f_{\parallel}$ axis that is caused by the slight up turn in pitch angle contours near 1.79 keV and 0°. This small effect should not necessarily be viewed as a real effect.

Another common feature of magnetosphere distribution functions that can be seen in Figures 13 and 14 is the existence of a low energy component of the plasma. Such a cold component is thought to be very important in controlling instabilities leading to the electrostatic electron cyclotron waves (Kennel and Ashour-Abdalla, 1982) which probably precipitate the particles of the diffuse aurora.

Discussion and Summary

A survey of the location of the inner edge of the plasma sheet surrounding the earth has confirmed most of the previously reported characteristics of this boundary and revealed several new features. The boundary is energy dependent with lower energy electrons penetrating closer to the earth. The low energy boundary is furthest from the earth in the dusk region and the 11 R_e distance given by Vasyliunas (1968a) is indeed a typical location in this region. The boundary is closer to the earth at local times approaching midnight and is often adjacent to the plasmapause, especially during disturbed conditions and at still later local times (see also Schield and Frank, 1970; Frank, 1971; Horwitz et al., 1982). In the dawn-noon sector the inner edge is beyond the average plasmapause distance only during quiet times. In the noon-dusk sector the boundary as seen on eccentric orbiting spacecraft is confined to a relativly narrow region between 11 R_e and the magnetopause (Vasyliunas, 1968b). At this location the boundary shows minimal energy dispersion and is frequently oscillating on a time scale of minutes.

Near midnight the inner edges at energies of several keV are often only a few tenths of an earth radius further from the earth than the low energy boundaries. Shielding is apparently important in this region. Near dawn and after dusk, however, this separation is frequently as large as several R_e. This is especially true near dawn where a simple cross-tail electric field model predicts the separation should be a minimum.

Several facts argue against the importance of strong diffusion near the inner edge of the plasma sheet. Comparing the close in locations near dawn to those expected if strong diffusion were operating (Kennel, 1969; Southwood and Wolf, 1978) shows that they are much closer to earth than they would be under

strong diffusion. For example, Southwood and Wolf (1978) indicate a boundary at 9 R_e for a relatively strong electric field of 2 keV/R_e whereas dawn boundaries are typically located near 5 R_e. We note, however, that inward convection of extended tail field lines will tend to produce an excess of plasma in the inner magnetosphere (Erickson and Wolf, 1980) whose precipitation might take longer and result in a somewhat more earthward inner edge. Additional arguments against strong diffusion come from the observations of anisotropic distribution functions that would otherwise be smoothed by strong diffusion. In various cases: (1) a depleted loss cone is seen at low altitudes; (2) enhanced fluxes are seen near 90° pitch angles near the equatorial plane; and (3) sharp depletions of 90° particles are seen near the inner edge.

Effects 2 and 3 above confirm predictions of models using the theory of single particle motion in a cross-tail electric field and dipole magnetic field. Even though data confirm these aspects of single particle theory, there are many problems with the simple model. Both the large separation at different energies mentioned above and the existence of a relativly thin plasma sheet near the dusk magnetopause are at variance with this model. A drastically different electric field model is probably needed.

Relatively good agreement between the ISEE measurements and those at low altitudes suggests that there is little reason to question the presumed correspondence between the inner edge of the plasma sheet and the low latitude boundary of the diffuse aurora. An exception to this statement may occur in the afternoon and dusk region where the low altitude data projected to the equatorial plane fall closer to the earth than the ISEE points near the magnetopause. An explanation to this discrepancy may be that ISEE sees the inner boundary of electrons convecting sunward from the dusk section of the tail while low altitude data detect a boundary of electrons that have arrived in the afternoon region via drift through dawn.

Incorporating our results with earlier proposals we arrive at the following explanation for the inner edge of the plasma sheet and the diffuse aurora. The cross-tail electric field causes earthward convection of plasma in the plasma sheet. The motion of electrons in the existing electric and

magnetic fields causes departures from Maxwellian distributions; adiabatic compression occurs but 90° pitch angle particles are energized more than field aligned electrons; eastward magnetic drifts are more important for higher energy electrons so that the higher energy electrons drift more rapidly eastward while lower energies penetrate closer to the earth. These anisotropies create free energy in the distribution functions which can lead to waves which scatter electrons into the loss cone and produce the diffuse aurora, but this process often does not proceed at the strong diffusion rate. The effects of the ionospheric portion of this system are also undoubtedly important. Shielding occurs (e.g., Southwood and Wolf, 1978) and any simple electric field will probably be substantially modified by all these effects. Plasma transport will undoubtedly occur along field lines and there is indeed evidence that a cool electron population mingles with the hot plasma sheet population. These cool electrons have important influences on the instability conditions that produce waves. Clearly this is a complex problem whose quantitative solution will undoubtedly require the simultaneous consideration of the many diverse aspects via a sophisticated computer model such as is being constructed at Rice University (e.g., Harel et al., 1982).

Acknowledgments

The authors express their appreciation to principle investigator K. W. Ogilvie for use of the ISEE electron data, to J. D. Scudder for help in understanding spacecraft and instrumental effects and for use of his sophisticated data reduction program and to R. J. Fitzenreiter for the use of his display programs. Thanks are also due to C. T. Russell for use of his magnetic field data. We also acknowledge useful discussions with many colleagues.

REFERENCES

Ashour-Abdalla, M., and S. W. H. Cowley, Wave particle interactions near the geostationary orbit, in Magnetospheric Physics, edited by B. M. McCormac, D. Reidel, Hingham, MA, 241-270, 1974.

Ashour-Abdalla, M., and C. F. Kennel, Diffuse auroral precipitation, J. Geomag. Geoelectr., 30, 239-255, 1978.

Berchem, J., and J. Etcheto, Experimental study of magnetospheric convection, Adv. Space Res., 1, 179-184, 1981.

Cowley, S. W. H., and M. Ashour-Abdalla, Adiabatic plasma convection in a dipole field: Variation of plasma bulk parameters with L., Planet. Space Sci., 23, 1527-1549, 1975.

Cowley, S. W. H., and M. Ashour-Abdalla, Adiabatic plasma convection in a dipole field: Electron forbidden zone effects for a simple electric field model, Planet. Space Sci., 24, 805-819, 1976.

Ejiri, M., Trajectory traces of charged particles in the magnetosphere, J. Geophys. Res., 83, 4798-4810, 1978.

Ejiri, M., R. A. Hoffman, and P. H. Smith, Energetic particle penetrations into the inner magnetosphere, J. Geophys. Res., 85, 653-663, 1980.

Erickson, G. M., and R. A. Wolf, Is steady convection possible in the earth's magnetotail?, Geophys. Res. Lett., 897-900, 1980.

Foster, J. G., C. G. Park, L. H. Brace, J. R. Burrows, J. H. Hoffman, E. F. Maier, and J. H. Whitaker, Plasmapause signatures in the ionosphere and magnetosphere, J. Geophys. Res., 83, 1175-1182, 1978.

Frank, L. A., Relationship of the plasma sheet, ring current, trapping boundary, and plasmapause near the magnetic equator and local midnight, J Geophys. Res., 76, 2265-2275, 1971.

Gussenhoven, M. S., D. A. Hardy, and W. J. Burke, DMSP/F2 electron observations of equatorward auroral boundaries and their relationship to magnetospheric electric fields, J. Geophys. Res., 86, 768-778, 1981.

Gussenhoven, M. S., D. A. Hardy, N. Heinemann, and E. Holeman, 1978 diffuse auroral boundaries and a derived auroral boundary index, Air Force Geophys. Lab. Pub. AFGL-TR-82-0398, Hanscom AFB Mass, 1982.

Hardy, D. A., W. J. Burke, M. S. Gussenhoven, N. Heinemann, and E. Holeman, DMSP/F2 electron observations of equatorward auroral boundaries and their relationship to the solar wind velocity and the north-south component of the interplanetary magnetic field, J. Geophys. Res., 86, 9961-9974, 1981.

Harel, M., R. A. Wolf, P. H. Reiff, R. W. Spiro, W. J. Burke, F. J. Rich, and M. Smiddy, Quantitative simulation of a magnetospheric substorm 1. Model logic and overview, J. Geophys. Res., 86, 2217-2214, 1981.

Horwitz, J. L., W. K. Cobb, C. R. Baugher, C. R. Chappell, L. A. Frank, T. E. Eastman, R. R. Anderson, E. G. Shelley, and D. T. Young, On the relationship of the plasmapause to the equatorward boundary of the auroral oval and to the inner edge of the plasma sheet, J. Geophys. Res., 87, 9059-9069, 1982.

Hultquist, B., H. Borg, L. A. Holmgren, H. Reme, A. Bahnsen, M. Jespersen, and G. Kremser, Quiet time convection electric field properties derived from the keV electron measurements at the inner edge of the plasma sheet by means of GEOS-2, Planet. Space Sci., 30, 261-283, 1982.

Kavanagh, L. D., J. W. Freeman Jr., and A. J. Chen, Plasma flow in the magnetosphere, J. Geophys. Res., 73, 5511-5519, 1968.

Kennel, C. F., Consequences of magnetospheric plasma, Rev. Geophys., 7, 379-419, 1969.

Kennel, C. F., and M. Ashour-Abdalla, Electrostatic waves and the strong diffusion of magnetospheric electrons, in Magnetospheric Plasma Physics, edited by A. Nishida, D. Reidel, Hingham, Mass, 245-344, 1982.

Kivelson, M. G., and D. J. Southwood, Approximations for the study of drift boundaries in the magnetosphere, J. Geophys. Res., 80, 3528-3534, 1975.

Kivelson, M. G., S. M. Kaye, and D. J. Southwood, The physics of plasma injection events, in Dynamics of the Magnetosphere, S-I. Akasofu ed., D. Reidel, Hingham, Mass, 385-405, 1980.

Linscott, G. R., and M. W. J. Scourfield, Observations of the plasmapause and diffuse aurora, Planet. Space Sci., 24, 299, 1976.

Mead, G. D. and D. H. Fairfield, A quantitative magnetospheric model derived from spacecraft magnetometer data, J. Geophys. Res., 80, 523-534, 1975.

Mauk, B. H. and C.-I. Meng, Characterization of geostationary particle signatures based on the injection boundary model, J. Geophys., Res., 3055-3071, 1983.

Meng, C. I., B. Mauk and C. E. McIlwain, Electron precipitation of evening diffuse aurora and its conjugate electron fluxes near the magnetospheric equator, J. Geophys. Res., 84, 2545-2558, 1979.

Nakai, H., and Y. Kamide, Response of nightside auroral-oval boundaries to the interplanetary magnetic field, J. Geophys. Res., 88, 4005-4014, 1983.

Ogilvie, K. W., J. D. Scudder, and H. Doong, The electron spectrometer experiment on ISEE-1, Trans. Geoscience, Electronics, GE-16, 261-265, 1978.

Schield, M. A., and L. A. Frank, Electron observations between the inner edge of the plasma sheet and the plasmapause, J. Geophys. Res., 75, 5401-5414, 1970.

Scudder, J. D., E. C. Sittler, and H. S. Bridge, A survey of the electron environment of Jupiter: A view from Voyager, J. Geophys. Res., 86, 8157, 1981.

Sharber, J. R., The continuous (diffuse) auroral and auroral-E ionization, in Physics of Space Plasmas, edited by T. Chang, B. Coppi and J. R. Jasperse, Scientific Publishers, Cambridge Mass, 1981.

Sheehan, R. E., and R. L. Carovillano, Characteristics of the equatorward auroral boundary near midnight determined from DMSP images, J. Geophys. Res., 83, 4749-4754, 1978.

Slater, D. W., L. L. Smith, and E. W. Klechner, Correlated observations of the equatorward diffuse auroral boundary, J. Geophys. Res., 85, 531-542, 1980.

Southwood, D. J. and S. M. Kaye, Drift boundary approximations in simple magnetospheric convection models, J. Geophys. Res., 84, 5773-5780, 1979.

Southwood, D. J., and M. G. Kivelson, An approximate analytic description of plasma bulk parameters and pitch angle anisotropy under adiabatic flow in a dipolar magnetospheric field, J. Geophys. Res., 80, 2069-2073, 1975.

Southwood, D. J. and R. A. Wolf, An assessment of the role of precipitation in magnetospheric convection, J. Geophys. Res., 83, 5227-5232, 1978.

Swift, D. W., Mechanisms for auroral precipitation: a review, Rev. Geophys. Space Phys., 19, 185-211, 1981.

Vasyliunas, V. M., A survey of low energy electrons in the evening sector of the magnetosphere with OGO-1 and OGO-3, J. Geophys. Res., 73, 2839-2884, 1968a.

Vasyliunas, V. M., Low energy electrons on the day side of the magnetosphere, J. Geophys. Res., 73, 7519-7523, 1968b.

Wrenn, G. L., J. F. E., Johnson, and J. J. Sojka, Stable "pancake" distributions of low energy electrons in the plasma trough, Nature, 279, 512-514, 1979.

Figure Captions

Fig. 1. Theoretical boundaries for the inner edge of the electron plasma sheet at 4 different energies. The curves are for a uniform cross tail electric field of .95 keV/R_e and they have been rotated -8° (clockwise) to fit the observed locations on July 17, 1983 shown as dots. The shaded region separates curves for electrons with pitch angles of 0° (inner curve) and 90° (outer curve).

Fig. 2a. Log f vs time for 14 energy channels on July 17, 1978. The flux decrease characteristic of the inner edge of the plasma sheet is seen first at the highest energy at 0330 and then later at lower energies with the lowest energy decrease occuring at 0500. The solid line represents the best fit theoretical inner edge for E = .95 kev/R_e and a -8° rotation as illustrated in Figure 1.

Fig. 2b. Electron density, pressure, average energy and anisotropy (log $P_{\parallel}/P_{\perp}$) are shown along with the measured magnetic field magnitude and direction angles. The direction of the principle axis of the pressure tensor is superposed on the magnetic field direction. Alignment of the two vectors occurs whenever a large enough anisotropy allows calculation of a meaningful pressure tensor axis. The inner edge manifests itself as an average energy decrease controled primarily by the high energies at 0330 and a density decrease controlled primarily by the low energies at 0445.

Fig. 3a. Similar to Fig. 2a only for the pre-noon region on December 7, 1978. The best fit electric field is E = .58 keV/R_e rotated -1.5°.

Fig. 3b. Similar to Fig. 2b only for the pre-noon region on December 7, 1978. Enhancement of 90° electrons at these local times frequently leads to a significant anisotropy and the good alignment of magnetic field and pressure tensor axis as shown.

Fig. 4a. Similar to Fig. 2a for the afternoon region on September 5, 1978. After passing through the magnetopause the spacecraft sees highly variable plasma sheet fluxes in a relativly narrow region near the magnetopause.

Fig. 4b. Similar to Fig. 2a for the afternoon region on September 5, 1978.

Fig. 5a. Similar to Fig. 2a only for inbound and outbound passes near dusk and midnight on February 11-12, 1978. The best fit electric field of E = .54 keV/R_e rotated 13° was obtained using both passes simultaneously. The relative poorness of the fit suggests deficiencies in the simple model.

Fig. 5b. Similar to Fig. 2b for data on February 11-12, 1978.

Fig. 6. Separation of inner edges at different energies. The dawn separations tend to be much larger than predicted by simple theoretical models.

Fig. 7a. Equatorial plane view of 1 keV inner edge locations on quiet days. Open circles represent outbound passes and solid circles represent inbound passes. Crosses representing magnetopause crossings are connected to their corresponding inner edge crossings by trajectory lines. Dashed lines indicate average low altitude positions of the low latitude boundary of the diffuse aurora which have been projected to the equatorial plane.

Fig. 7b. Similar to Fig. 7a only for disturbed conditions. Large solid circles now represent inbound inner edge crossings for disturbed times. Small solid circles indicate all the quiet inner edges reproduced from Fig. 7a for reference.

Fig. 8. A revised version of Fig. 2 of Vasyliunas (1968b) showing a schematic view of the inner edge of the plasma sheet in the equatorial plane. Hypothetical flow patterns have been added in an attempt to reconcile the afternoon boundary measurements by OGO and ISEE near the

magnetopause with those of ATS and SCATHA near the synchronous orbit. Dots represent the relative intensity of plasma sheet fluxes.

Fig. 9. Panels showing log f vs pitch angle at 12 different energies. Each panel illustrates the crossing of the inner edge at a different energy on June 20, 1978. The energy whose boundary is being crossed is characterized by an obvious depletion of particles near 90°.

Fig. 10. Panels similar to Fig. 9 only illustrating inner edge crossings at 510 eV on four different days in the evening quadrant.

Fig. 11. Panels similar to Fig. 9 which display a 90° peak that appears to be supperposed on a distribution that would otherwise have maxima at 0/180° pitch angles and a minimum at 90°. It is suggested that the 90° peak may result from the preferential acceleration of such particles drifting in a dipole-like field.

Fig. 12. Panels similar to Fig. 9; only from the dawn region near the equatorial plane.

Fig. 13. Contours of the electron distribution function are shown above orthogonal cuts through the distribution. Heavy lines in the lower panel indicate $f_{\parallel}$ and lighter lines $f_{\perp}$ while the dots indicate one count levels of the various measured energy channels. In the upper panels the dots indicate the location of the measurements in $v_{\parallel}$, $v_{\perp}$ space.

Fig. 14. Plots of the types shown in Figures 9 and 13 are combined for times when the spacecraft cut auroral L shells at relativly low altitudes. Evidence for an empty loss cone can be seen, particularly in panels a and c.

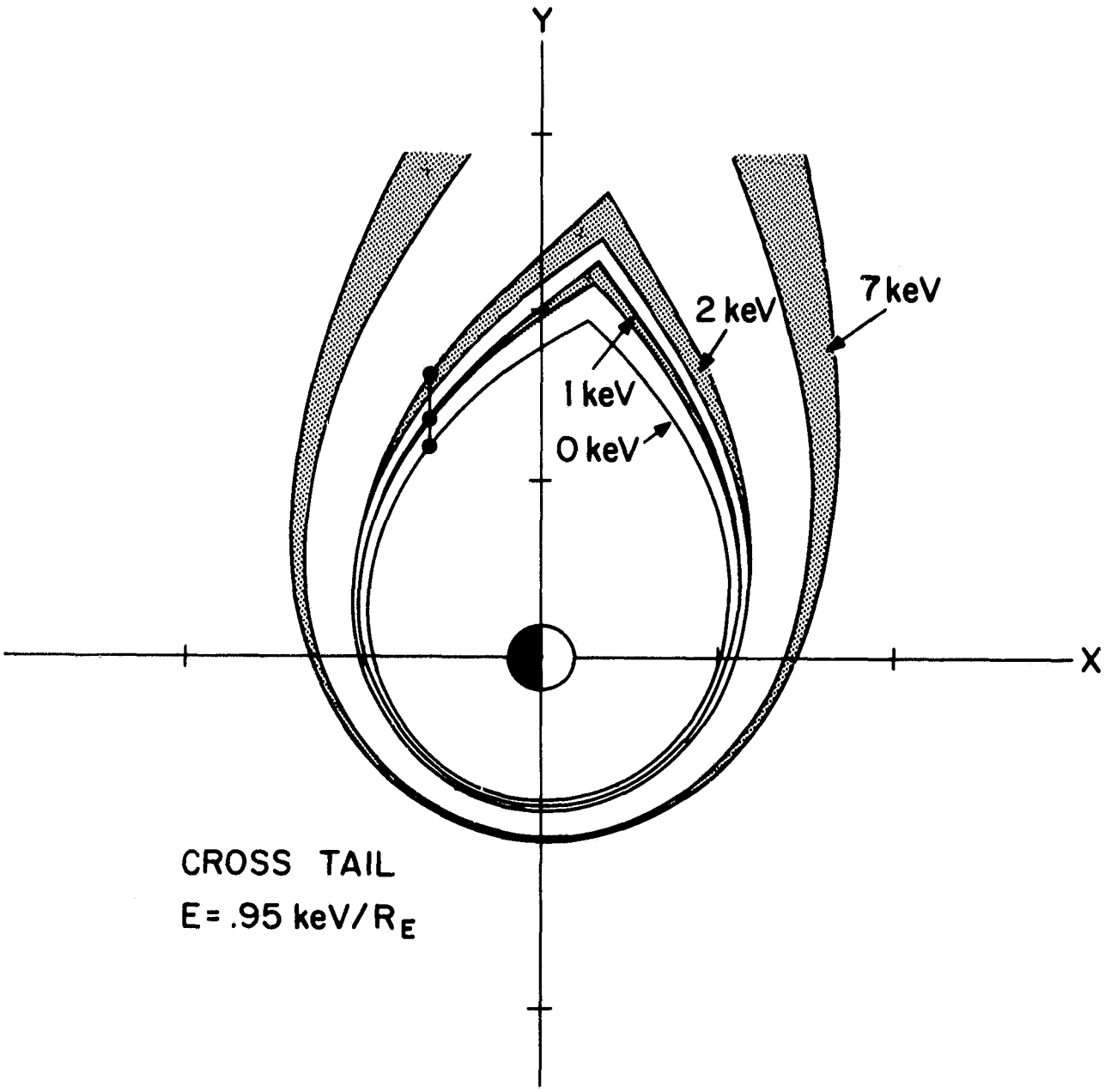

Figure 1

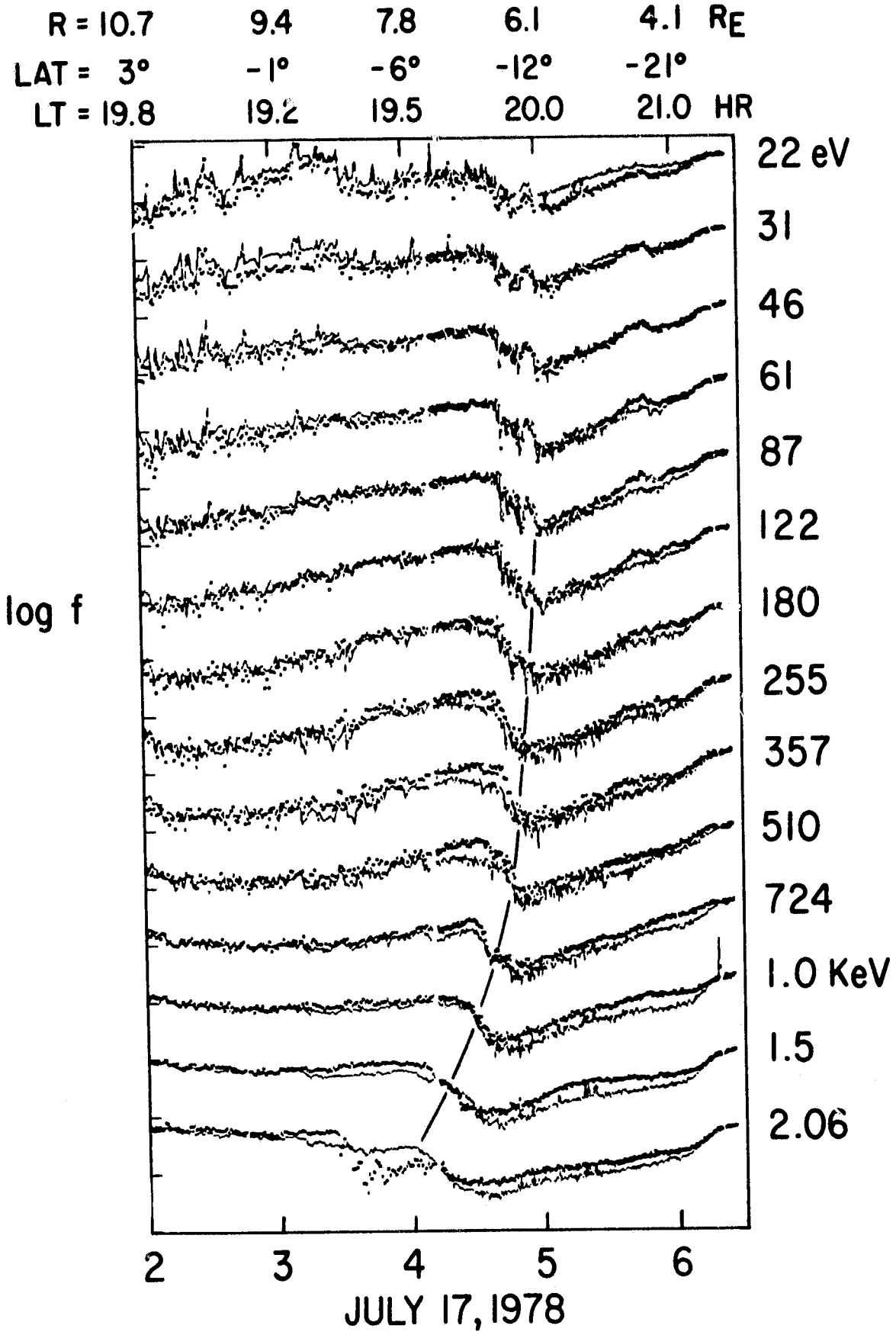

Figure 2a

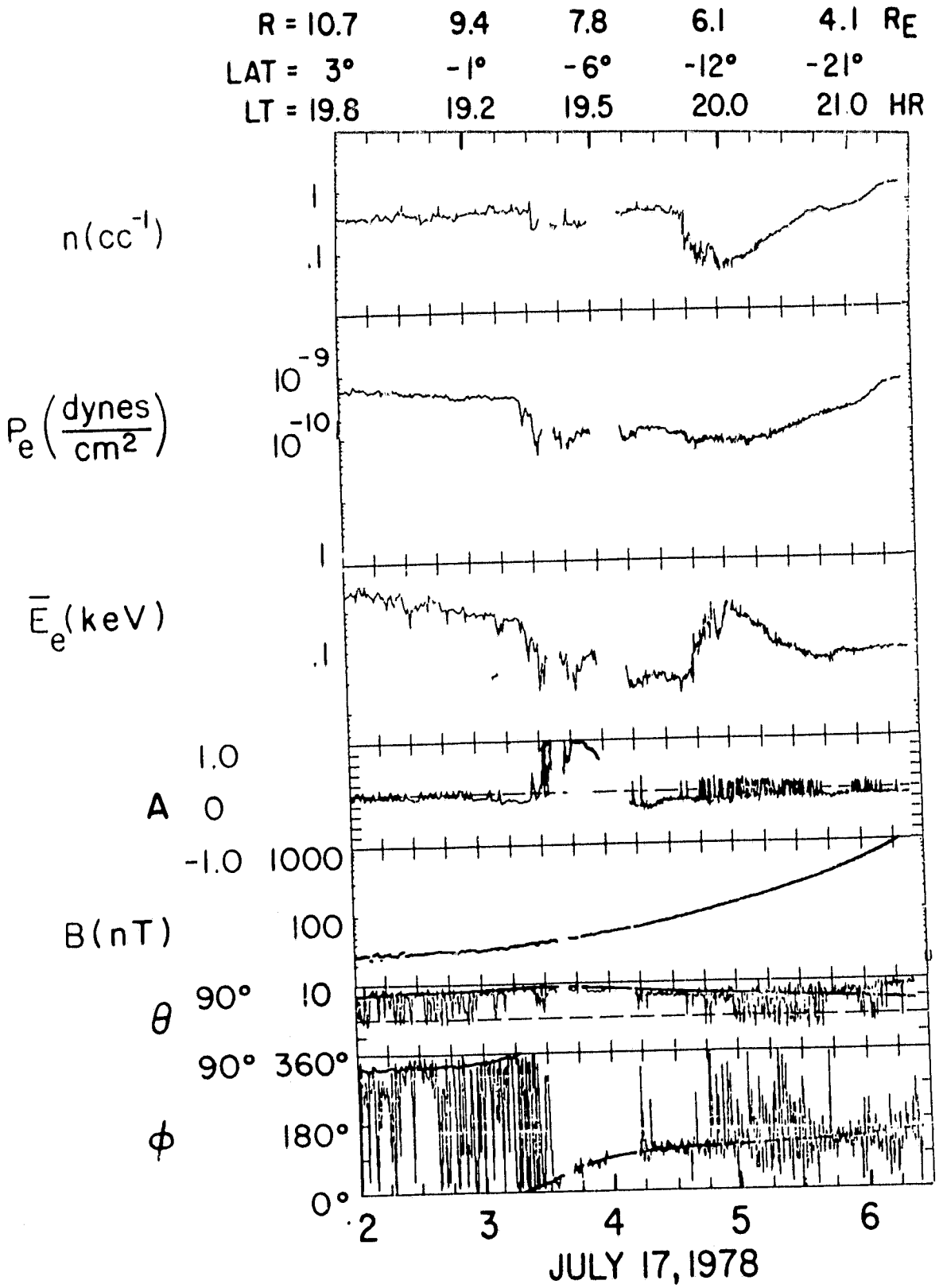

Figure 2b

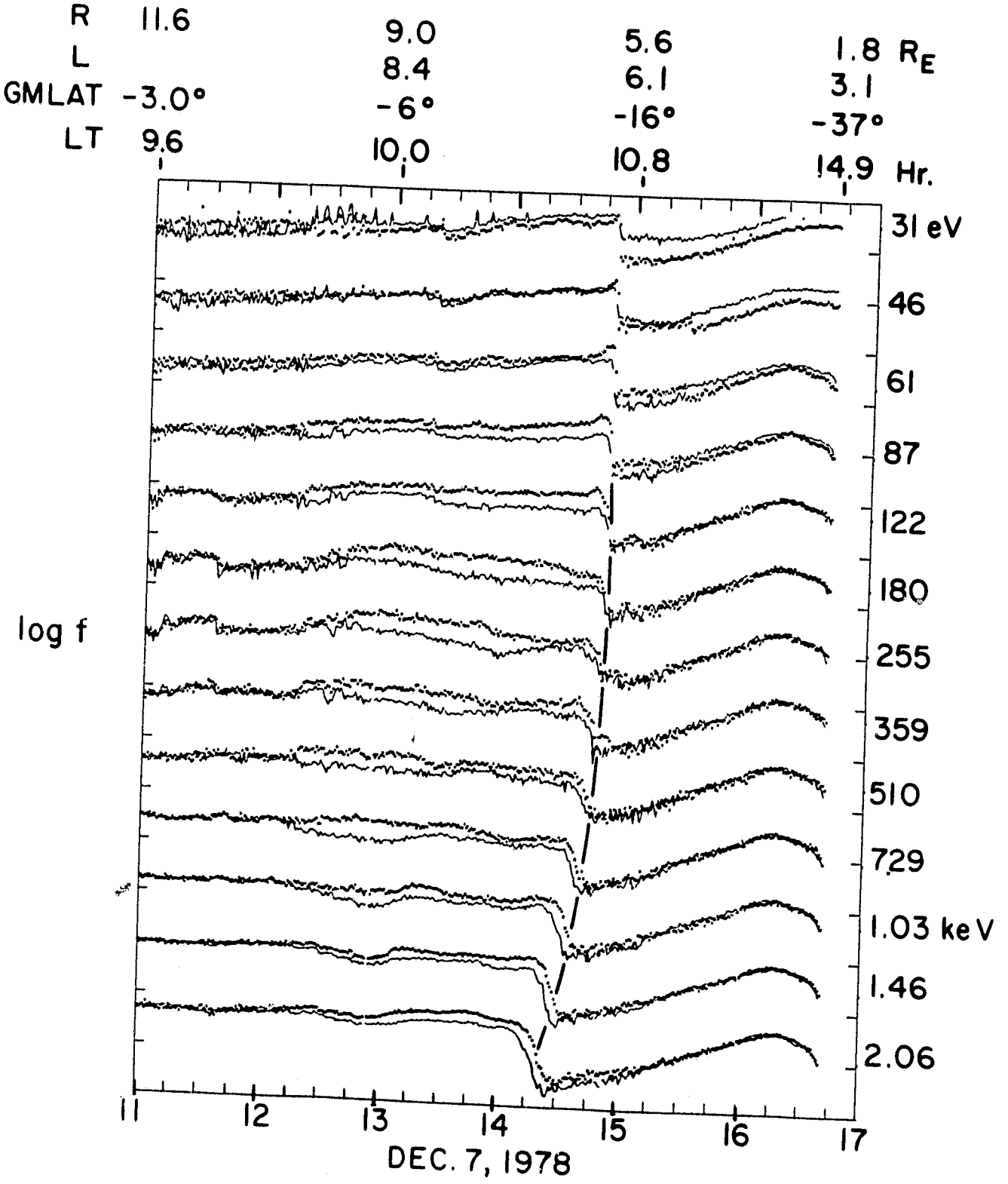

Figure 3a

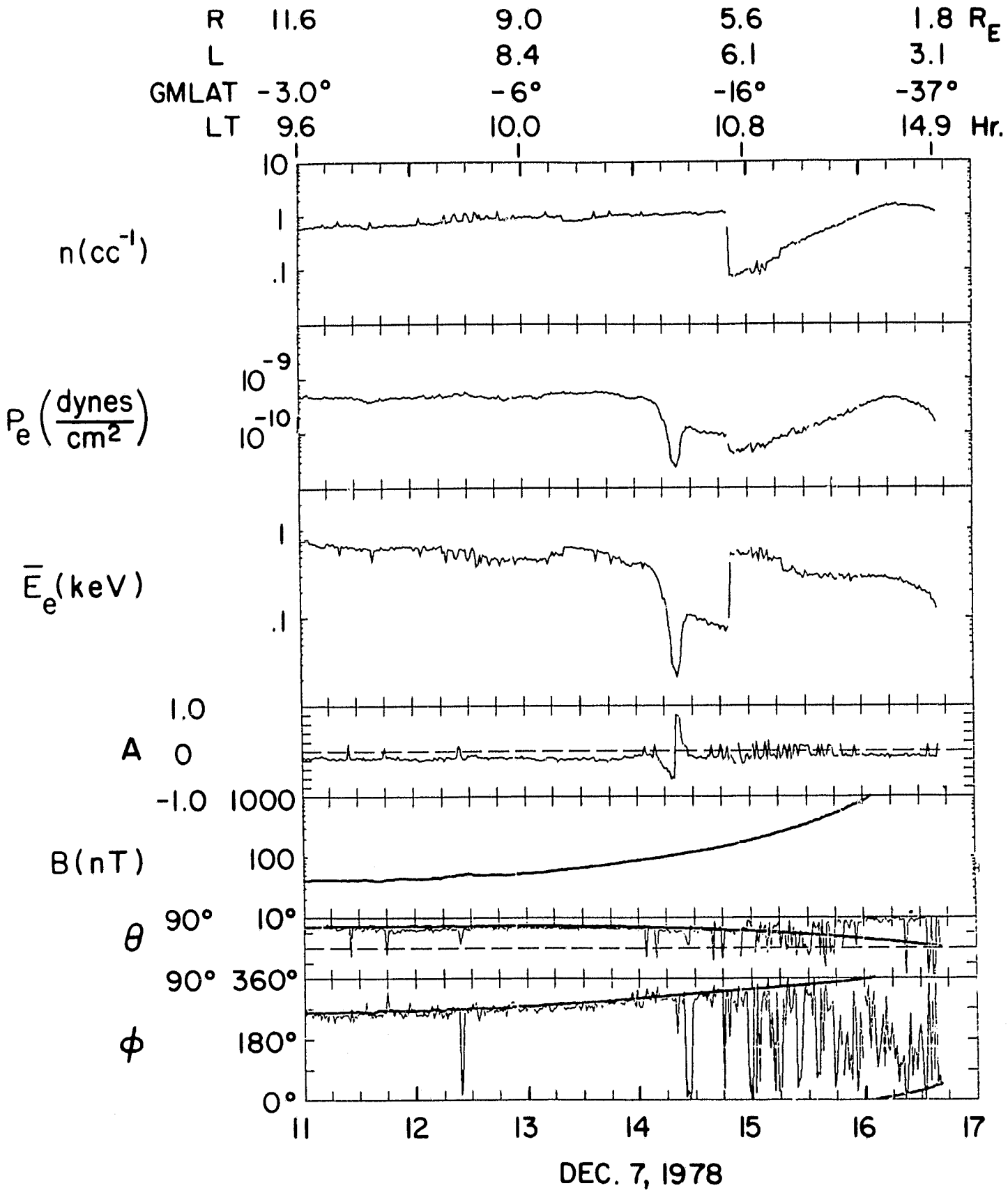

Figure 3b

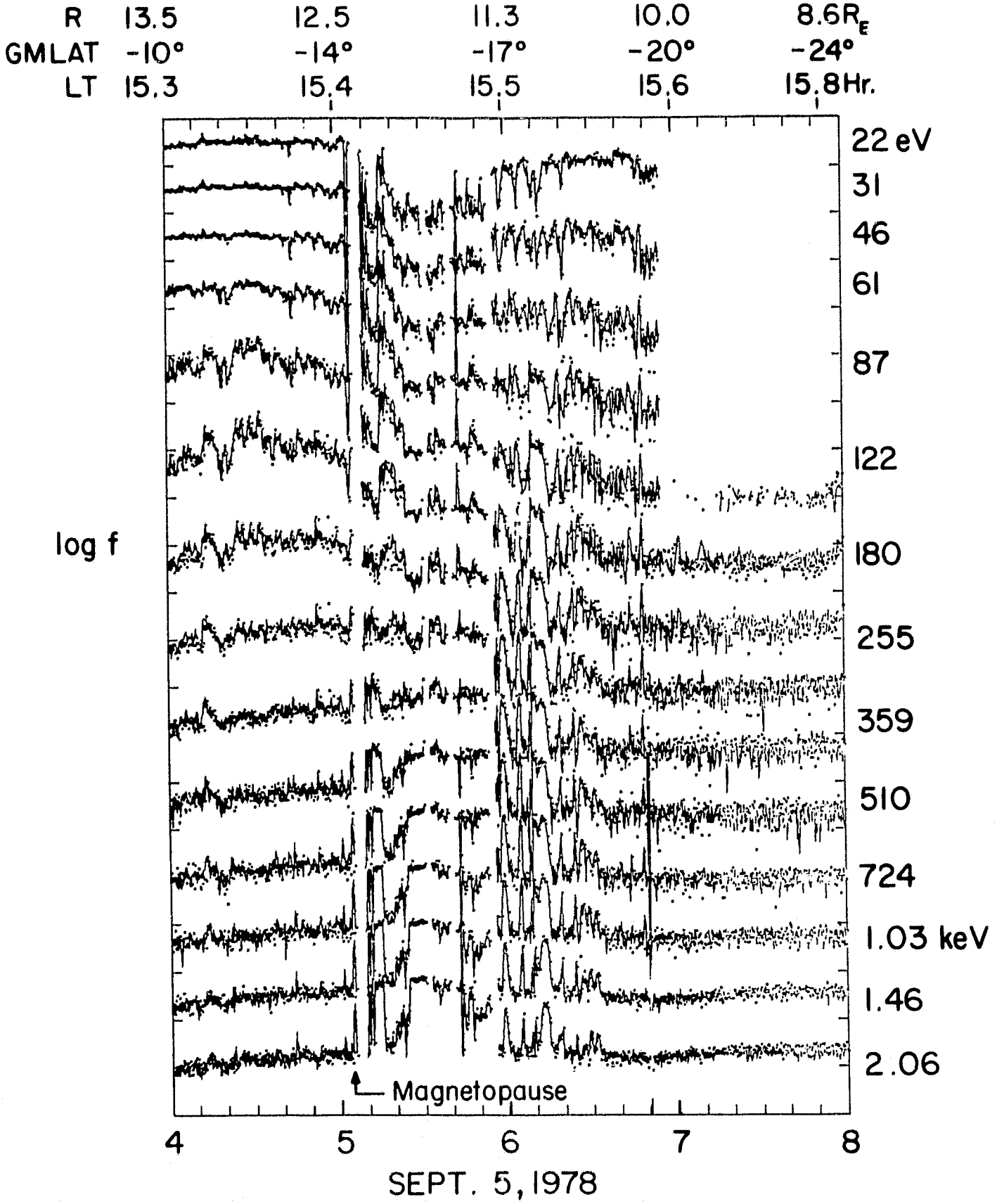

Figure 4a

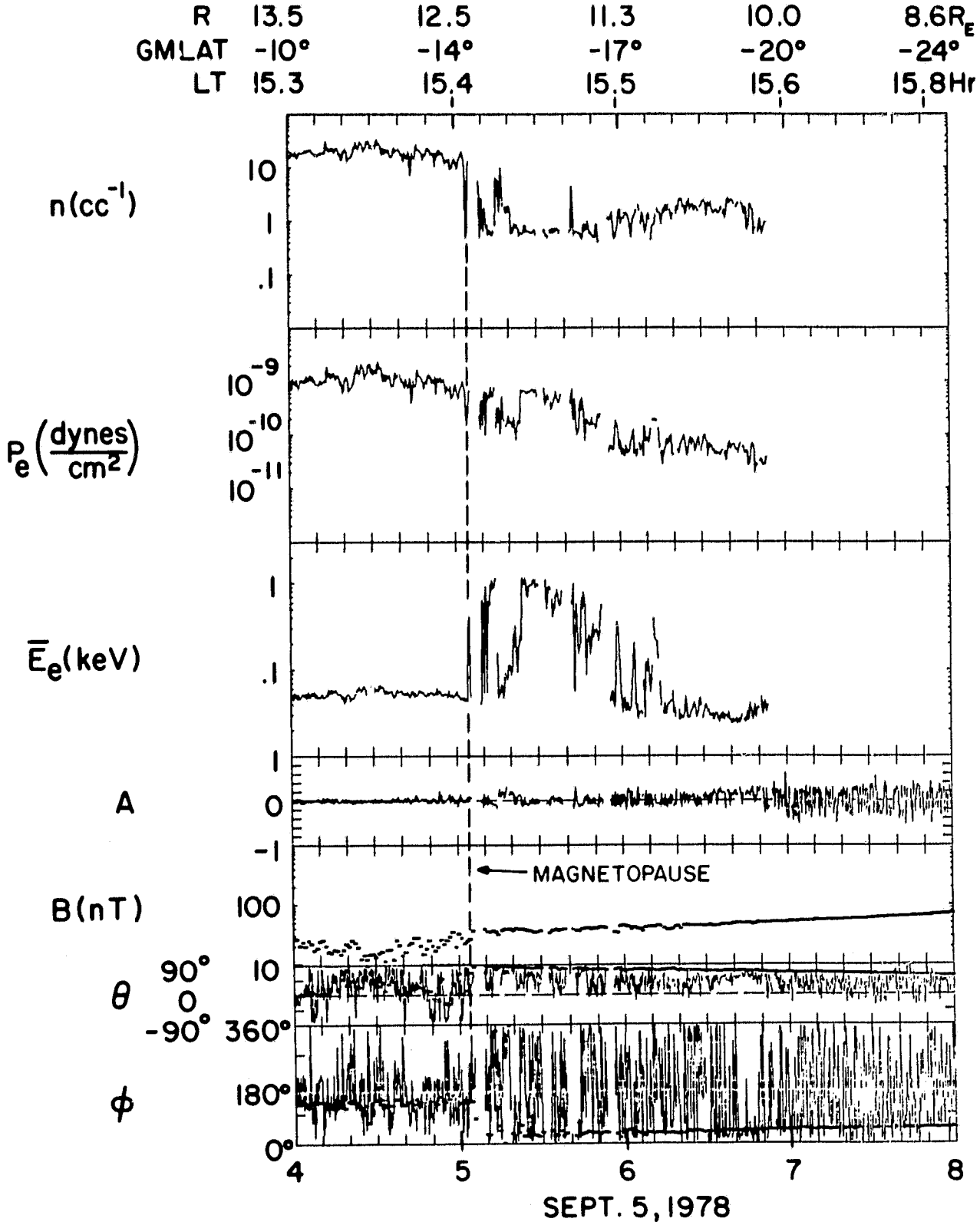

Figure 4b

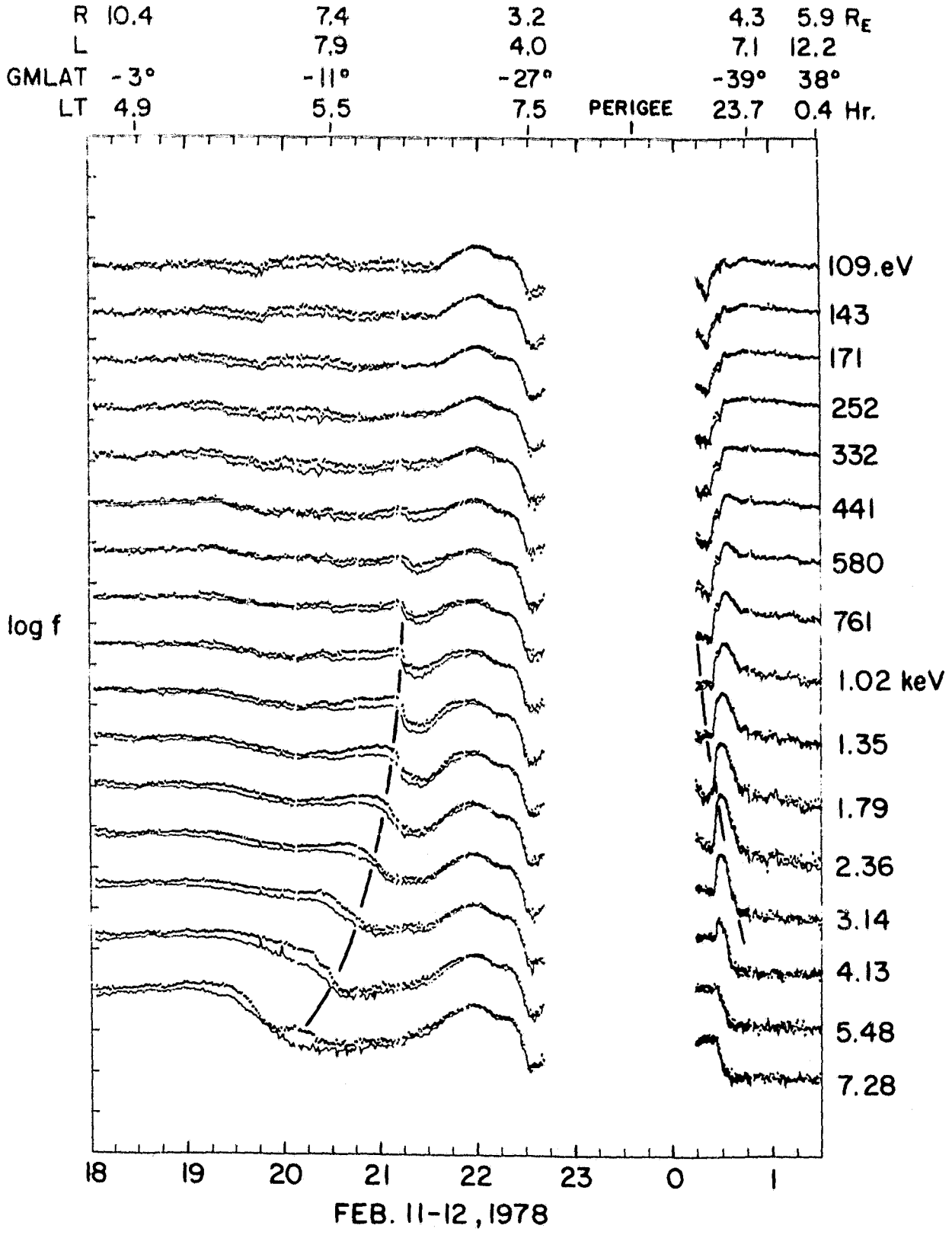

Figure 5a

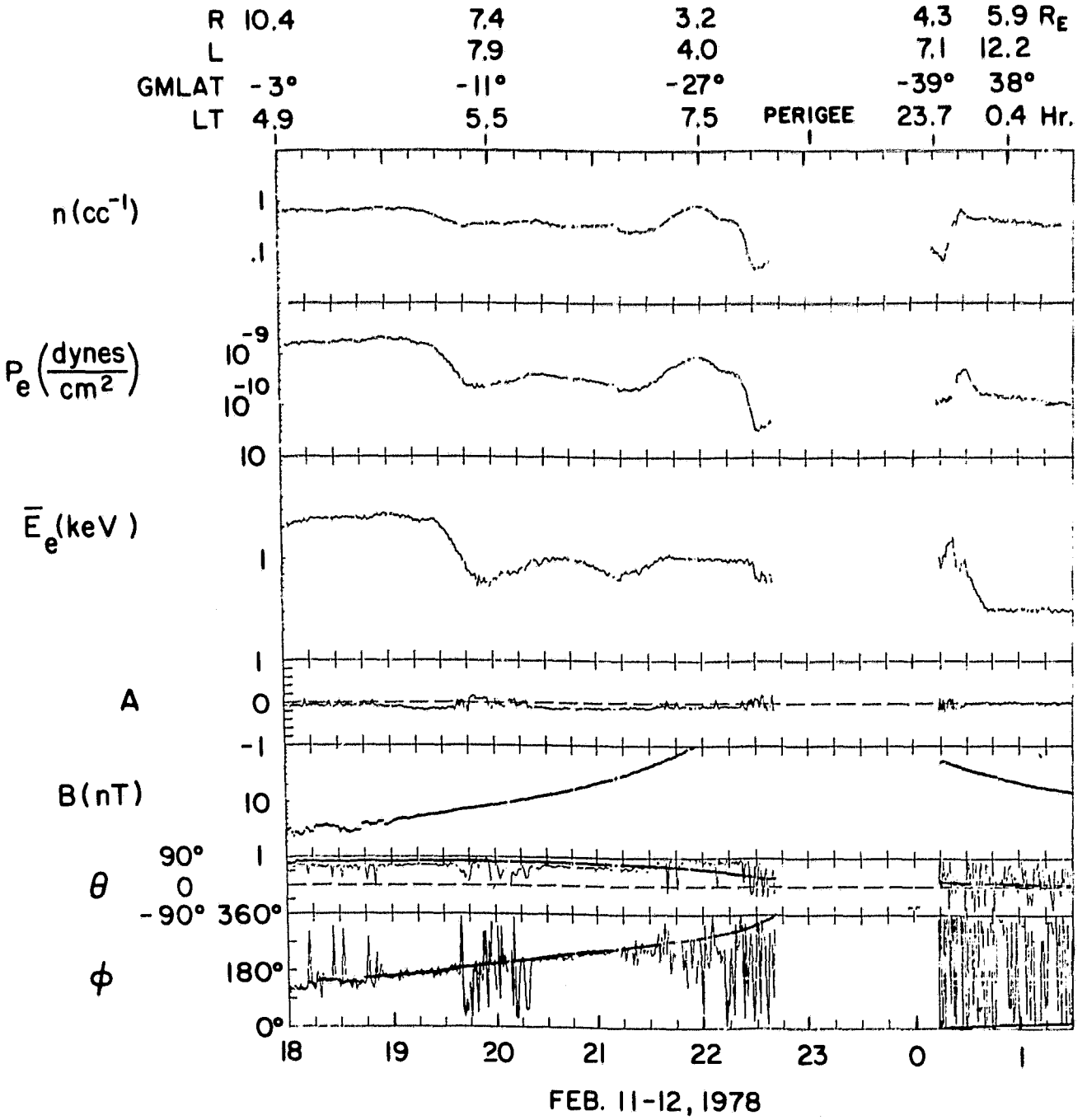

FEB. 11-12, 1978

Figure 5b

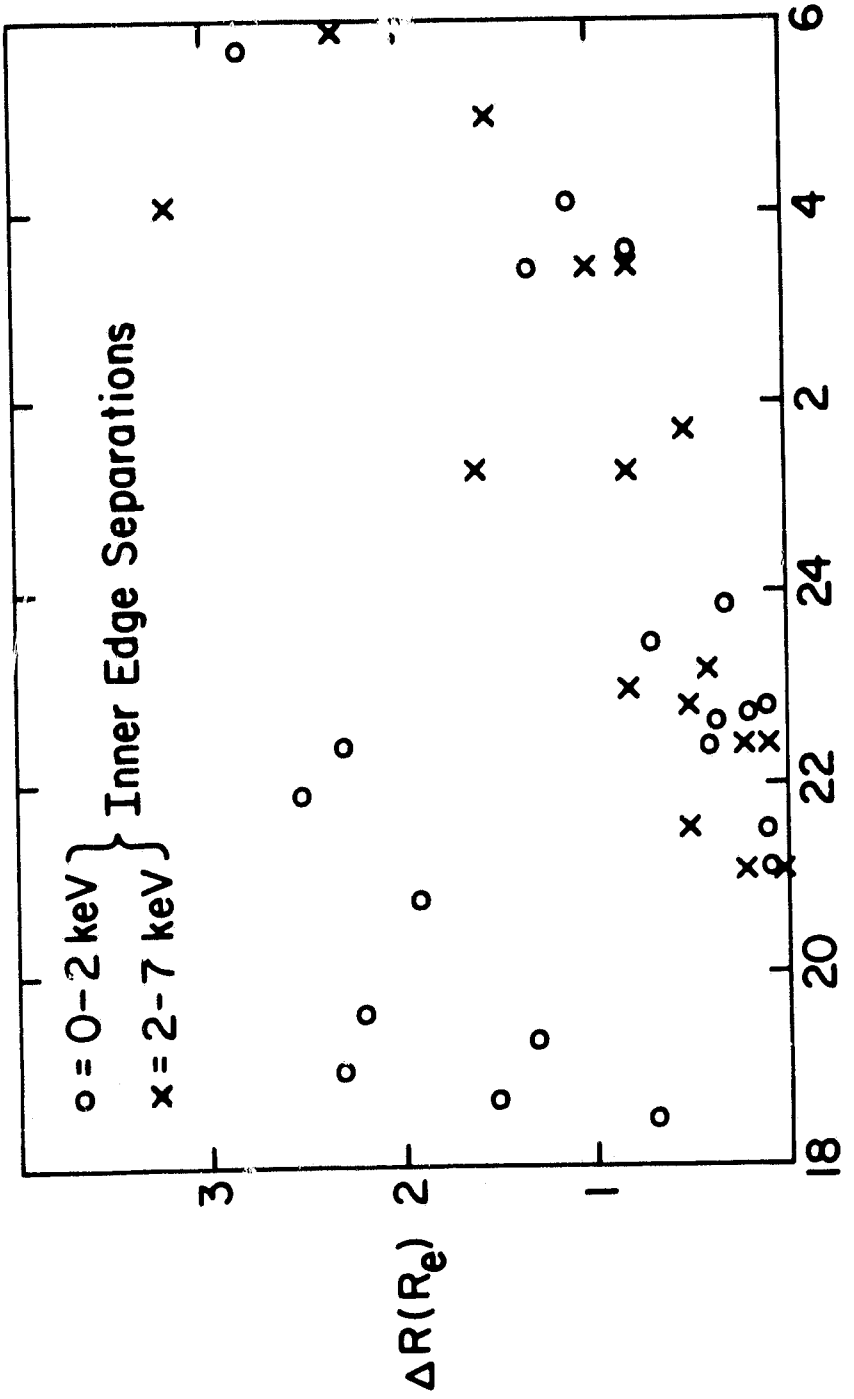

Figure 6

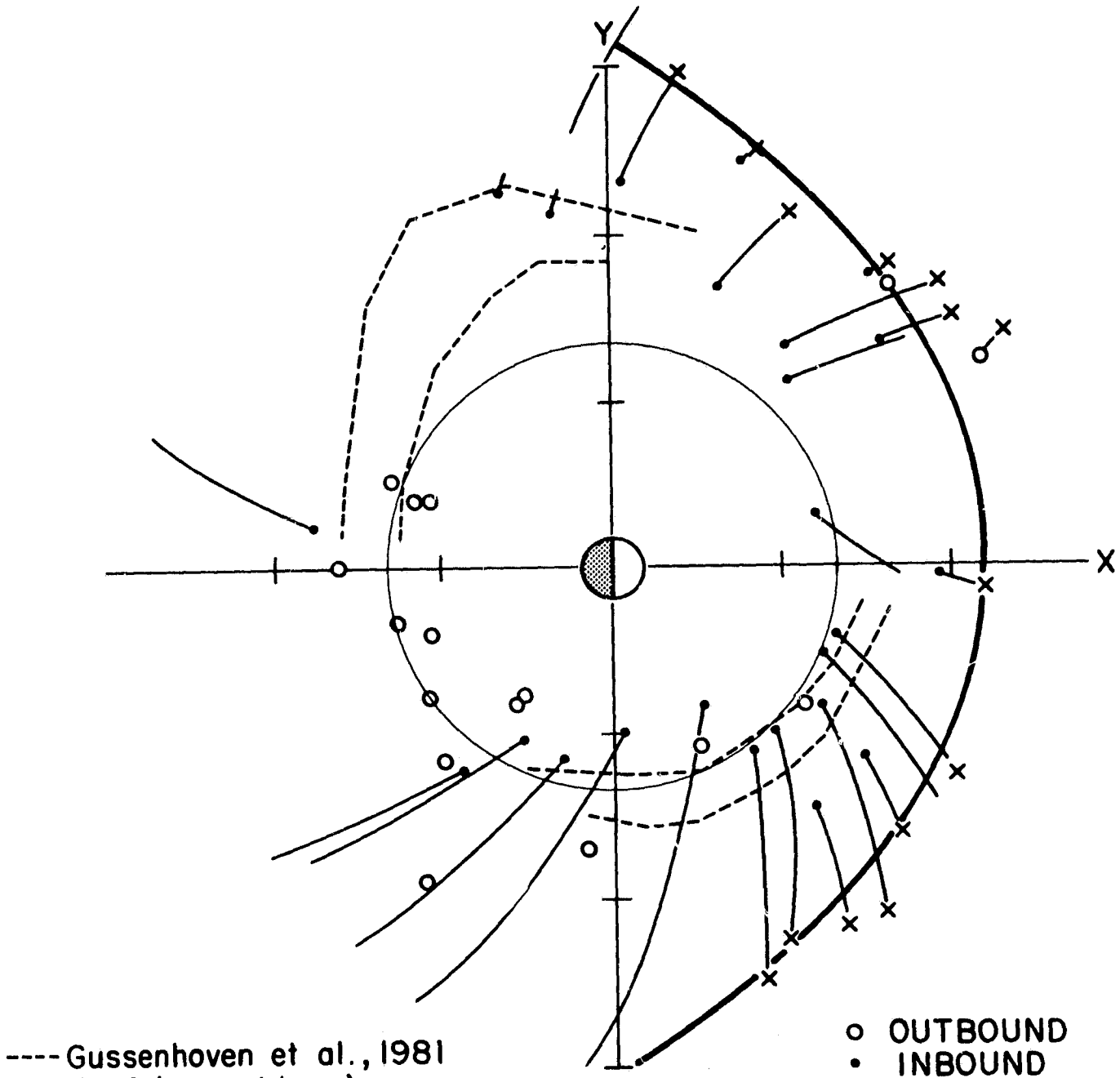

Figure 7a

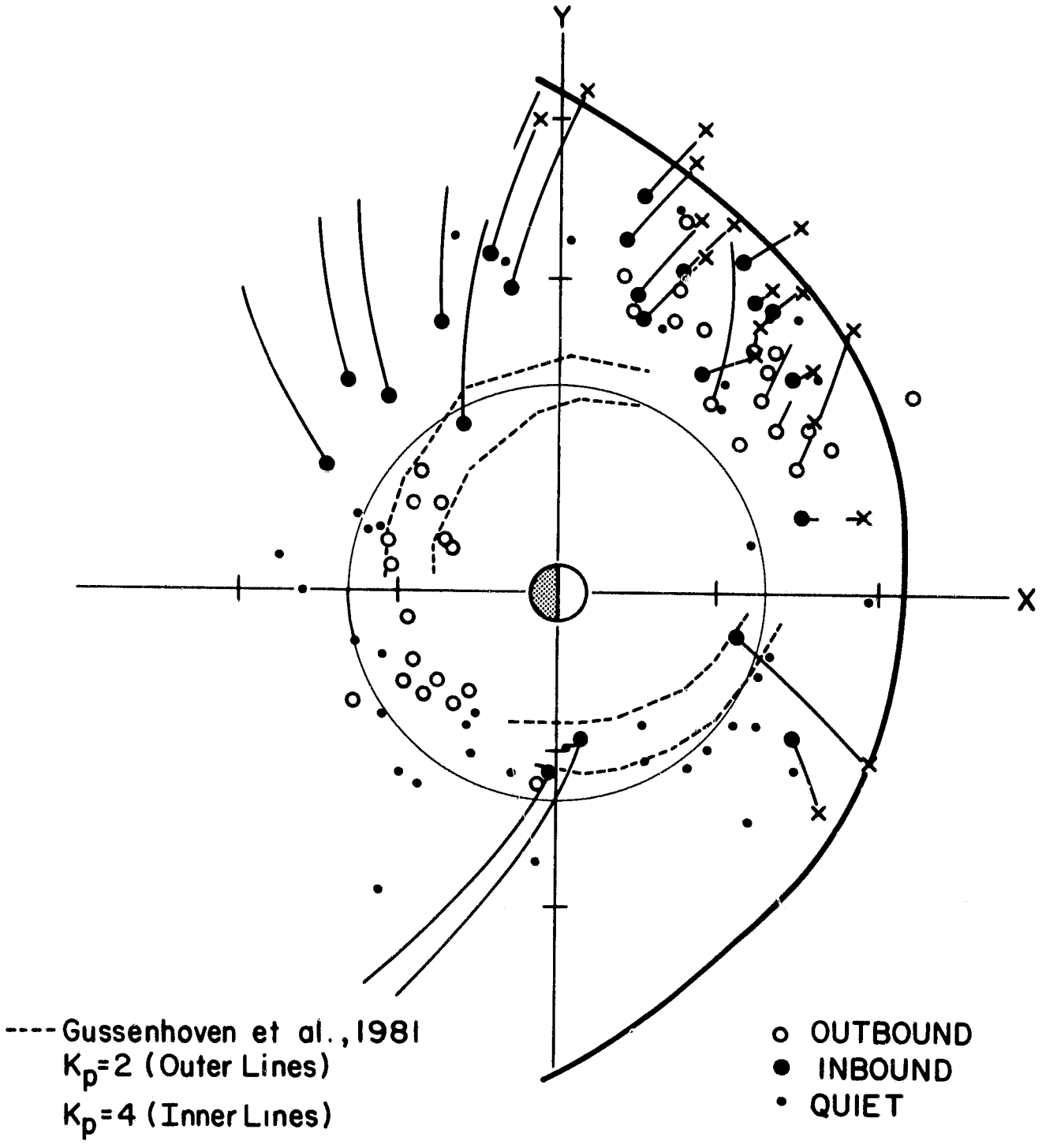

Figure 7b

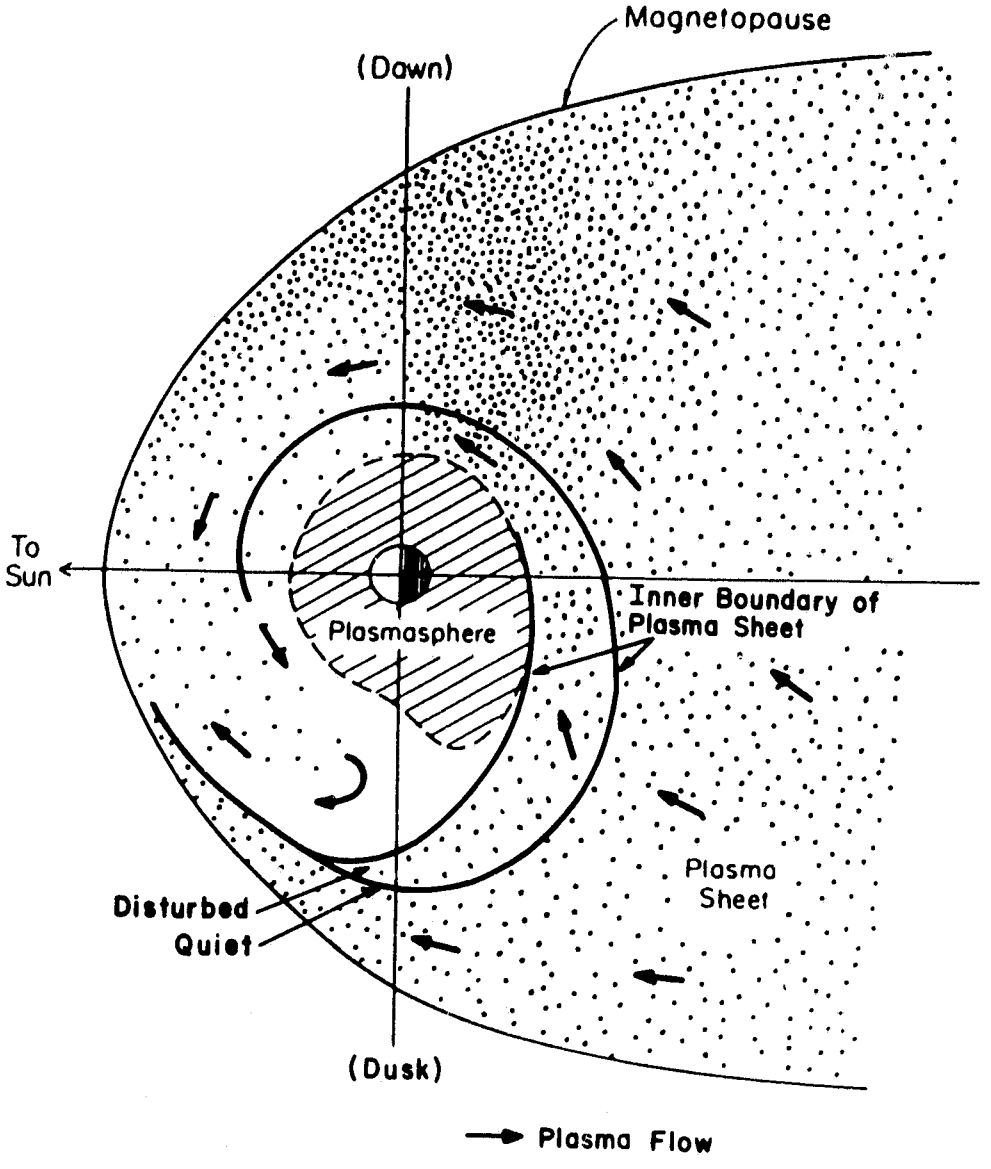

Figure 8

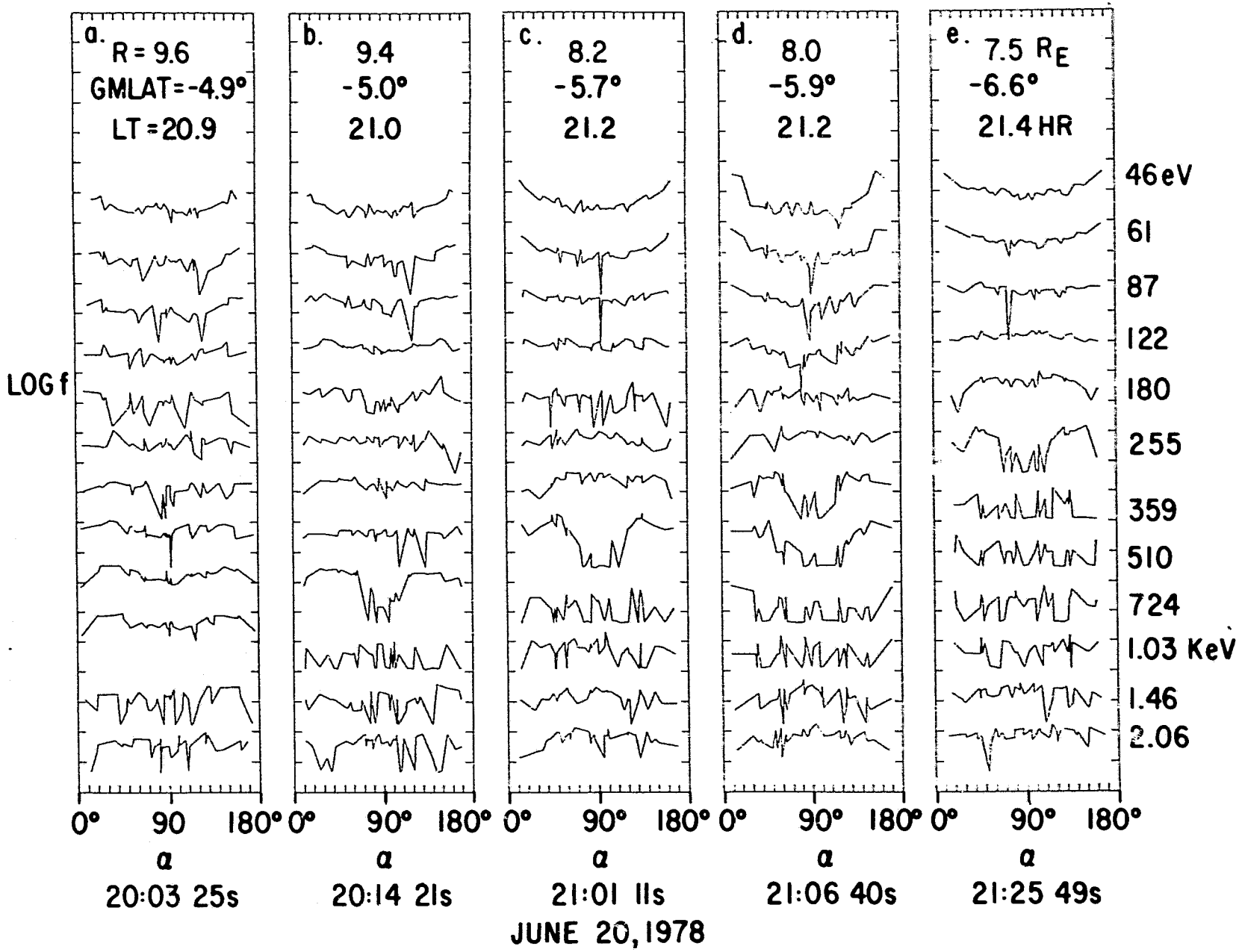

Figure 9

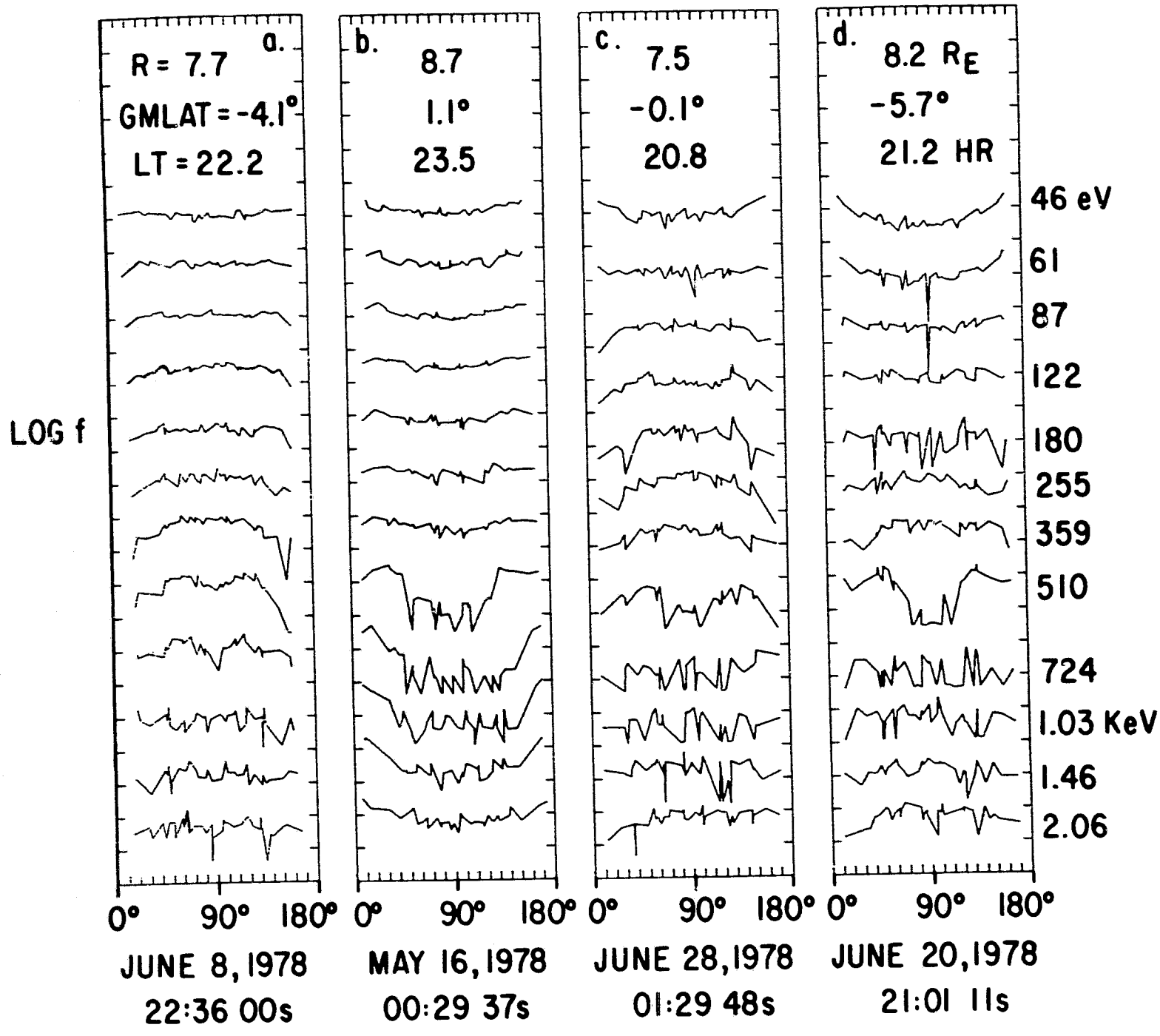

Figure 10

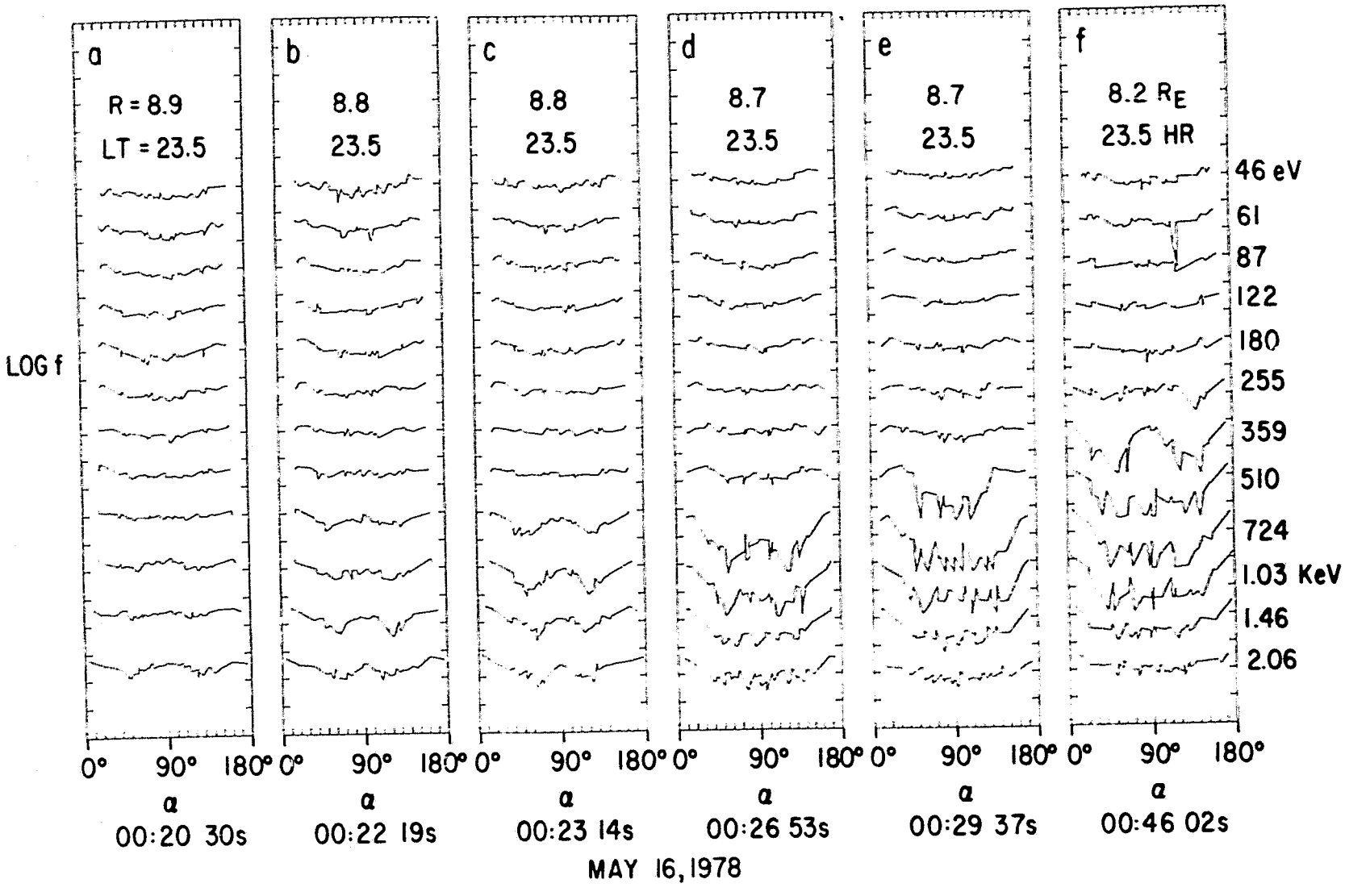

Figure 11

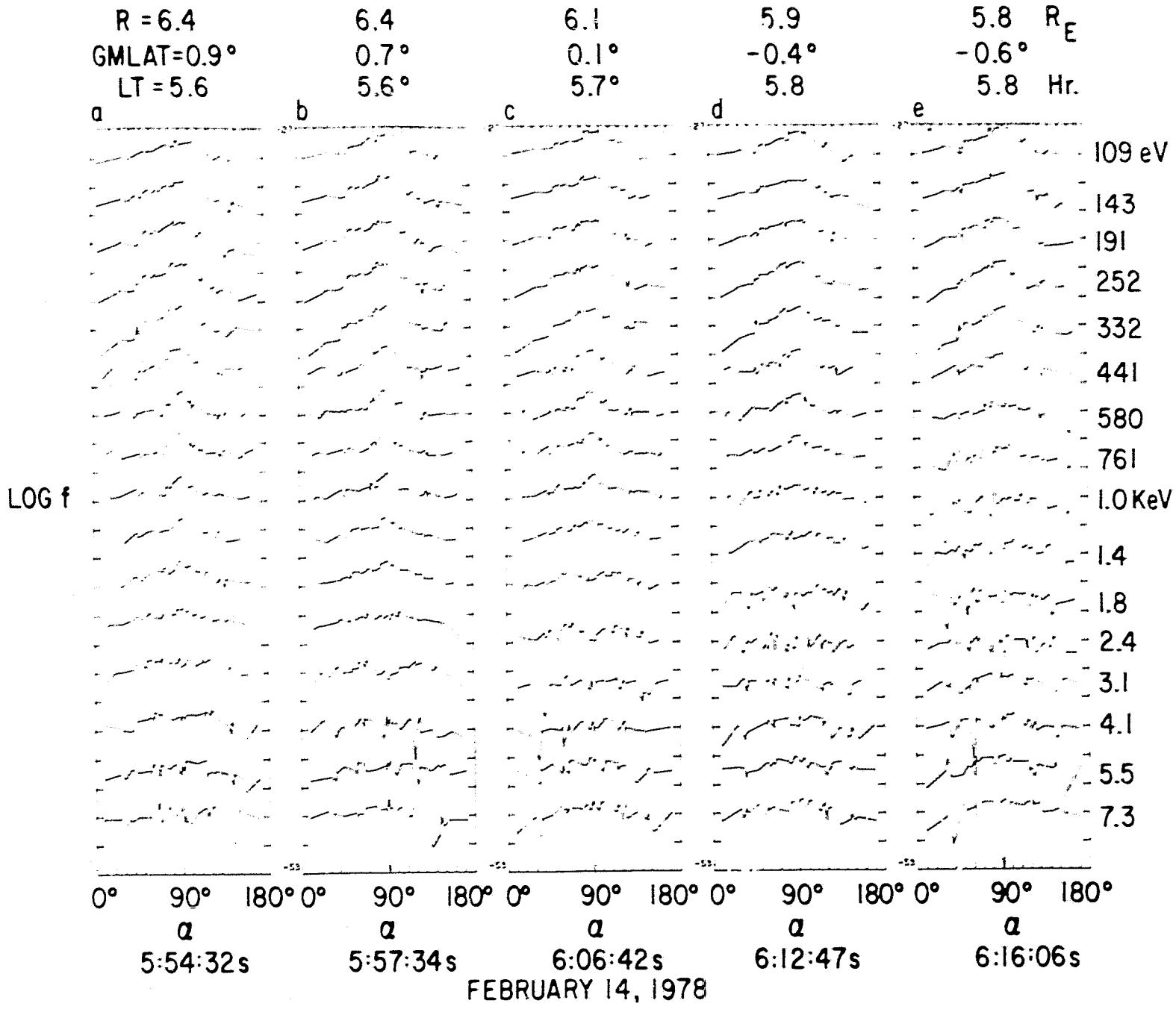

Figure 12

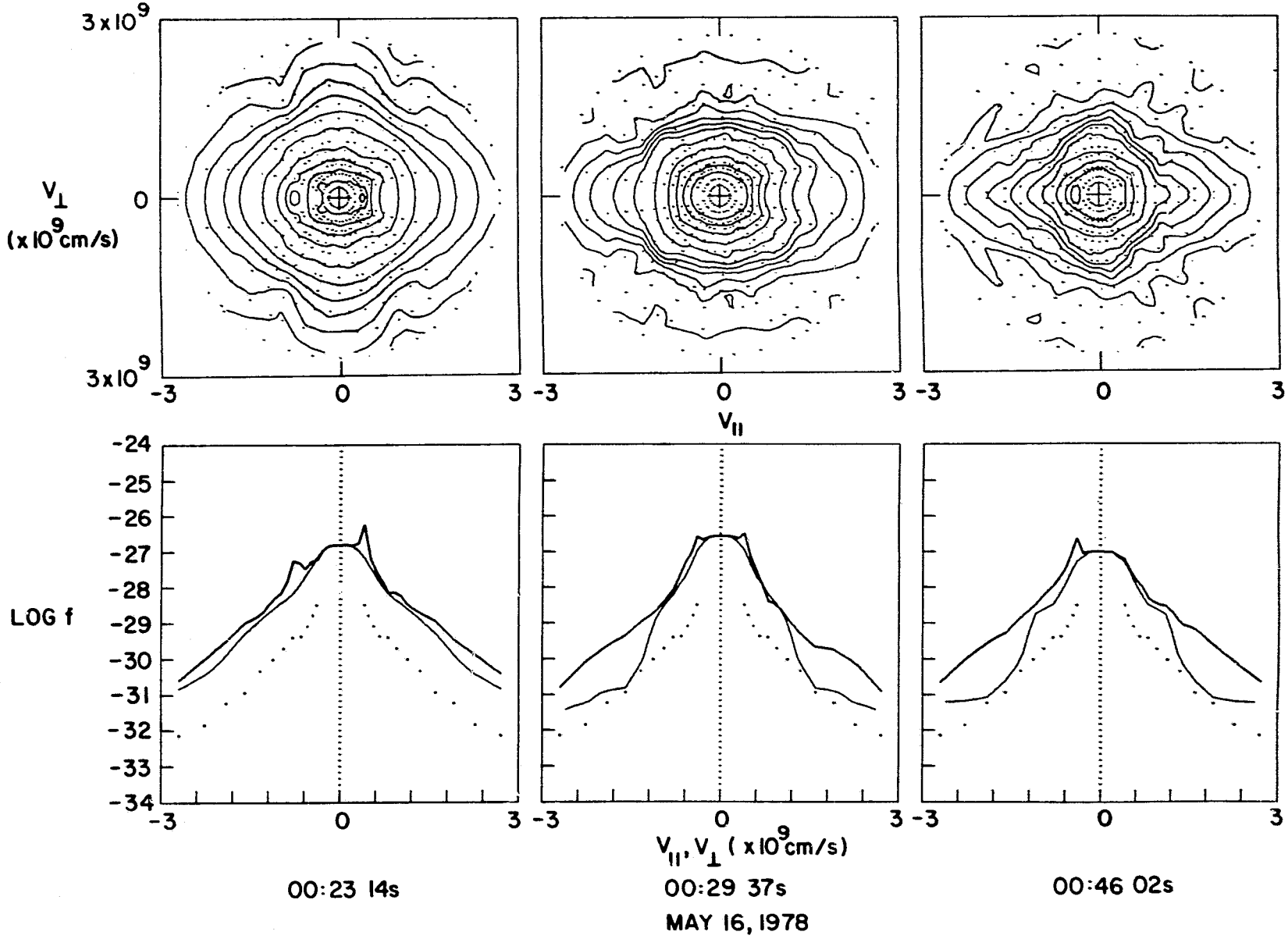

Figure 13

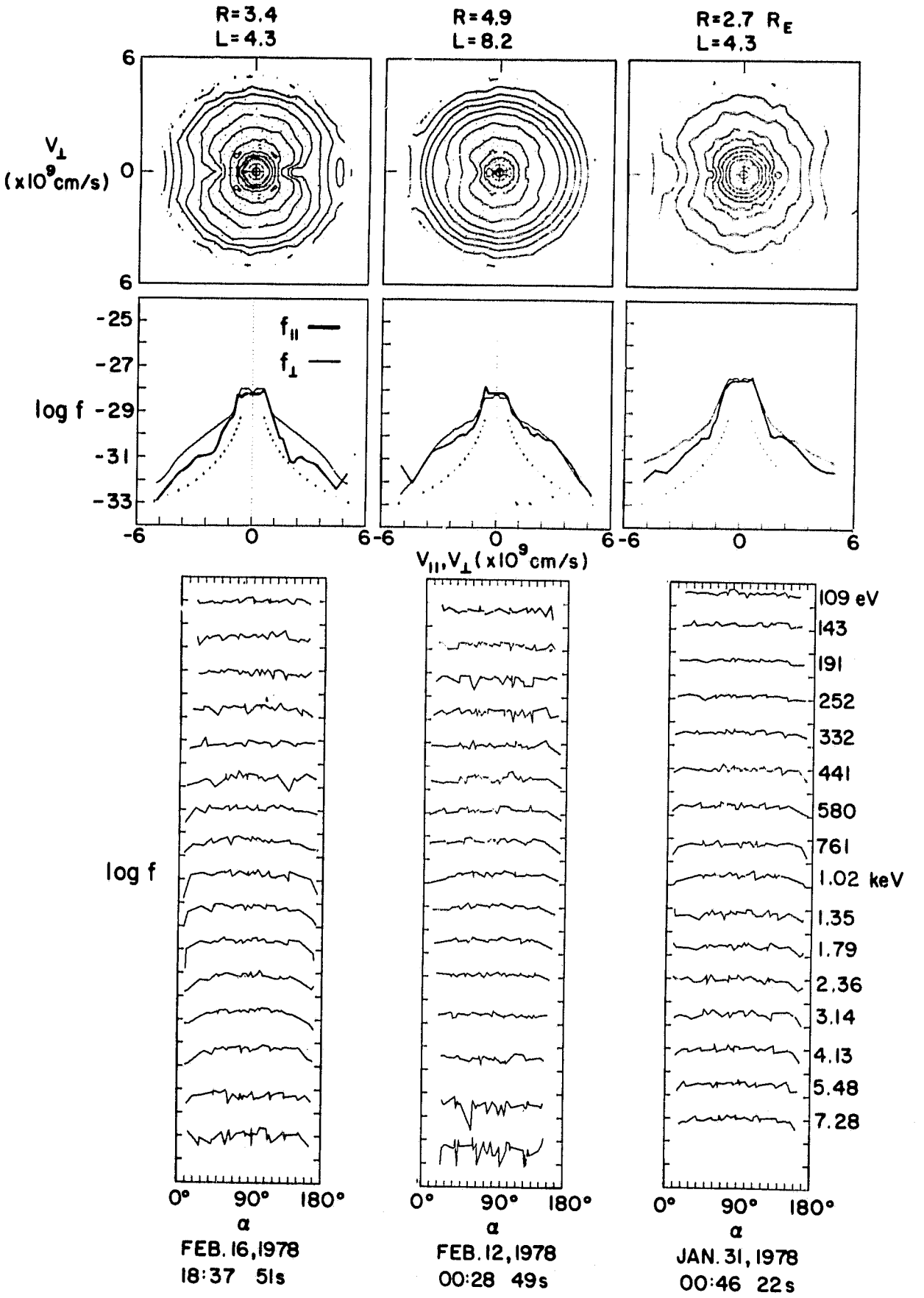

Figure 14